AD

AD-E403 081

Contractor Report ARAET-CR-06001

DEVELOPMENT OF CO-EXTRUSION TECHNOLOGIES FOR GREEN MANUFACTURE OF ENERGETICS

Professor Dilhan M. Kalyon
Dr. Halil Gevgilili
Dr. Hansong Tang
Dr. Moinuddin Malik
Arshad Mirza
E. Deminkol
Dr. Bert Greenberg
Stevens Institute of Technology
Highly Filled Materials Institute
Castle Point on Hudson
Hoboken, NJ 07030

Ducan Park
Kristin Jasinkiewicz
Judith M. Mahon
Project Engineers
ARDEC

April 2006

ARMAMENT RESEARCH, DEVELOPMENT AND ENGINEERING CENTER

Armaments Engineering & Technology Center

Picatinny Arsenal, New Jersey

The views, opinions, and/or findings contained in this report are those of the author(s) and should not be construed as an official Department of the Army position, policy, or decision, unless so designated by other documentation.

The citation in this report of the names of commercial firms or commercially available products or services does not constitute official endorsement by or approval of the U.S. Government.

Destroy this report when no longer needed by any method that will prevent disclosure of its contents or reconstruction of the document. Do not return to the originator.

REPORT DOCUMENTATION PAGE	*Form Approved OMB No. 0704-01-0188*

1. REPORT DATE (DD-MM-YYYY)	2. REPORT TYPE	3. DATES COVERED (*From - To*)
April 2006		

4. TITLE AND SUBTITLE	5a. CONTRACT NUMBER
DEVELOPMENT OF CO-EXTRUSION TECHNOLOGIES FOR GREEN MANUFACTURE OF ENERGETICS	DAAE30-00-D-1011-DO #23-2
	5b. GRANT NUMBER
	5c. PROGRAM ELEMENT NUMBER

6. AUTHORS	5d. PROJECT NUMBER
D. M. Kalyon, H. Gevgilili, H. Tang, M. Malik, A. Mirza, E. Deminkol, and B. Greenberg SIT Duncan Park, Kristin Jasinkiewicz, and Judith M. Mahon, Project Engineers, ARDEC	5e. TASK NUMBER
	5f. WORK UNIT NUMBER

7. PERFORMING ORGANIZATION NAME(S) AND ADDRESS(ES)	8. PERFORMING ORGANIZATION REPORT NUMBER
Stevens Institute of Technology Highly Filled Materials Institute Castle Point on Hudson Hoboken, NJ 07030 U.S. Army ARDEC, AETC Energetics, Warheads & Environmental Technology (AMSRD-AAR-AEE-W/E) Picatinny Arsenal, NJ 07806-5000	

9. SPONSORING/MONITORING AGENCY NAME(S) AND ADDRESS(ES)	10. SPONSOR/MONITOR'S ACRONYM(S)
U.S. Army ARDEC, EM Technical Research Center (AMSRD-AAR-EMK) Picatinny Arsenal, NJ 07806-5000	11. SPONSOR/MONITOR'S REPORT NUMBER(S) Contractor Report ARAET-CR-06001

12. DISTRIBUTION/AVAILABILITY STATEMENT

Approved for public release; distribution is unlimited.

13. SUPPLEMENTARY NOTES

14. ABSTRACT

The manufacturing of co-extruded grains of highly filled propellant suspensions is a complicated operation, which requires a detailed and realistic understanding of the various types of interface, surface, and bulk instabilities. This understanding is necessary to be able to successfully manufacture fast core propellants using co-extrusion (ram or twin screw extrusion based). In this investigation, the fundamentals of the co-extrusion process were investigated by a combination of experimental and simulation studies. The project included the development of a novel experimental apparatus, which was used to investigate various types of flow instabilities and to collect basic data on various aspects of the fundamentals of the co-extrusion process. Furthermore, an analytical model of the process was developed by Prof. Kalyon at allow the determineation of the pressure drop versus flow rate relationships along with the velocity and shear stress distributions when two fluids are co-extruded side by side. The viscoplasticity and the wall slip of the two suspensions could be accommodated. The agreement between the theory and the experimental results was acceptable. In this final report, the techniques and the results obtained are outlined along with a listing of the reports and presentations that were made and a list of the lessons learned.

15. SUBJECT TERMS

Co-extrusion, Cc-extruded, ETPE, TPE, Energetic thermoplastic elastomer, PDMS, Polydimethyl siloxane, Fast core propellant, Co-layered, Wall slip, Shear stress, Mathematical modeling, Rheological, and Rheology

16. SECURITY CLASSIFICATION OF:			17. LIMITATION OF ABSTRACT	18. NUMBER OF PAGES	19a. NAME OF RESPONSIBE PERSON
a. REPORT	b. ABSTRACT	c. THIS PAGE			Duncan Parks, et al
U	U	U	SAR		19b. TELEPHONE NUMBER (Include area code) (973) 724-4398

CONTENTS

FIGURES

FIGURES
(continued)

SUMMARY

The manufacturing of co-extruded grains of highly filled propellant suspensions is a complicated operation, which requires a detailed and realistic understanding of the various types of interface, surface, and bulk instabilities. This understanding is necessary to be able to successfully manufacture fast core propellants using co-extrusion (ram or twin screw extrusion based). In this investigation, the fundamentals of the co-extrusion process were investigated by a combination of experimental and simulation studies. The project included the development of a novel experimental apparatus, which was used to investigate various types of flow instabilities and to collect basic data on various aspects of the fundamentals of the co-extrusion process. Furthermore, an analytical model of the process was developed by Prof. Dilhan M. Kalyon of the Stevens Institute of Technology (SIT), Hoboken, New Jersey to allow the determination of the pressure drop versus flow rate relationships along with the velocity and shear stress distributions when two fluids are co-extruded side by side. The viscoplasticity and the wall slip of the two suspensions could be accommodated. The agreement between the theory and the experimental results was acceptable. In this final report, the techniques and the results obtained are outlined along with a listing of the reports and presentations (refs. 1 through 8) that were made and a list of the lessons learned.

BACKGROUND AND OBJECTIVES

The manufacturing of co-extruded grains of highly filled propellants is a complicated operation, which requires a realistic understanding of the various types of interface, surface, and bulk instabilities. This understanding is necessary to be able to successfully manufacture fast core propellants using co-extrusion (ram or twin screw extrusion based). In this investigation, a novel experimental apparatus was developed and used to investigate various types of flow instabilities and to collect basic data on various aspects of the fundamentals of the co-extrusion process. Furthermore, an analytical model of the process was developed by Prof. Kalyon to allow the determination of the pressure drop versus flow rate relationships along with the velocity and shear stress distributions when two fluids are co-extruded side by side. The viscoplasticity and the wall slip of the two suspensions could be accommodated. In this final report, the techniques and the results obtained are outlined along with a listing of the reports and presentations that were made.

EXPERIMENTAL SET-UP

A modified ram extrusion process was used to generate various types of co-extruded grains using polydimethyl siloxane (PDMS) and suspensions of PDMS with hollow glass spheres, with the experiments designed to probe the different types of instabilities, which develop during the co-extrusion process (figs. 1 to 6). Various typical results obtained with differing combinations of fluids (the combination of pure binder on one side and a suspension on the other side is the most difficult and combinations of suspensions are easier to handle since the elasticity and shear viscosity differences are not as pronounced as in pure binder on one side of the co-extrusion die) are shown in figures 7 to 18. These results were elucidated in detail in our presentations and progress reports (refs. 1 through 8) and thus will not be detailed here.

Conclusions from the Experimental Studies

The experimental results outlined in our earlier results indicate that differences in the shear viscosity of the different phases, which are used in the co-extrusion process, affect the development of various types of interface and surface irregularities. If the shear viscosity material functions of the two phases are close to each other, then the effects of various types of instabilities are minimized.

On the other hand, if the differences in the shear viscosity material functions of the two phases are significant, then the ram extrusion process generates a time dependent change in the interface configuration along with differences in the surface irregularities of the two sides of the rectangular extrudates. **Thus, one of the major challenges of the selection of the different phases to be used in the fast core propellants will be to match the shear viscosity material functions of the fast and slow burn propellants by correct selection of temperatures and shear rate distributions in the co-extrusion hardware.** Some of the important issues in the design of the hardware are also identified.

MATHEMATICAL MODEL OF THE CO-EXTRUSION PROCESS

An analytical mathematical model of the co-extrusion of two suspensions flowing side by side in a co-extrusion die, subject to the viscoplasticity of the suspensions and their slip at the walls of the co-extrusion die was derived by Prof. Kalyon. The basic tenets of this model are described next:

- There are two suspensions that are viscoplastic which are flowing side by side in a slit die (fig. 19). This is the same geometry that is used in our experiments and is the most common general configuration, the modifications of which will provide the other configurations including the slow/fast/slow configuration.

- Both of the suspensions are subject to wall slip (fig. 20) at the walls of the co-extrusion die.

- The flow is isothermal and fully-developed (fig. 21) and contains multiple zones of deforming and non-deforming zones (figs. 22 through 24). Since the constitutive equation differs on shear stress less than the yield stress and the shear stress greater than the yield stress, and since the case of increasing velocity as the distance increases versus the case of decreasing velocity as the distance increases need to be treated separately multiple cases need to be addressed (fig. 25).

- The two fluids are incompressible.

The solutions indicate that there are twelve cases that are possible and each of these cases requires a separate solution. The simplifications of the model presented here would also include as a subset the flow of a single suspension subject to viscoplasticity and wall slip in a slit die. The 12 cases are shown in figure 25.

In the following the equations of the velocity distributions, shear stress distribution, the nomenclature and the differentiators between the twelve cases are provided for future documentation and the use of ARDEC. The derivation is novel and will be published with ARDEC acknowledgement and permission in the future.

Nomenclature

τ_{01} = Yield stress value of fluid 1
τ_{02} = Yield stress value of fluid 2
m_1 = the consistency index, fluid 1
m_2 = the consistency index, fluid 2
n_1 = power law index, fluid 1
n_2 = power law index of fluid 2
s_1 = $1/n_1$ is the reciprocal power-law index of fluid 1
s_2 = $1/n_2$ is the reciprocal power-law index of fluid 2
β_1 = Navier's slip coefficient for fluid 1
β_2 = Navier's slip coefficient for fluid2
y_i = distance of the interface from the wall

Subscript

y = y-direction
z = z-direction (flow direction)

Superscript

I = deformation zone for fluid 1
II = plug flow zone for fluid 1
III = first deformation zone for fluid 2
IV = plug flow zone for fluid2
V = second deformation zone for fluid 2

Equations used:

$$\tau_{yz} = \pm\tau_0 - m\left|\frac{dV_z}{dy}\right|^{n-1}\left(\frac{dV_z}{dy}\right)$$

$$\Lambda_1 = -\left[-\frac{dp}{dz}\frac{1}{m_1}\right]^{s_1}\frac{1}{s_1+1}$$

$$\Lambda_2 = -\left[-\frac{dp}{dz}\frac{1}{m_2}\right]^{s_2}\frac{1}{s_2+1}$$

The assumptions made for these derivations are:

- Fully developed flow
- Isothermal conditions
- The wall slip at both the wall is different
- The fluid is a viscoplastic and is represented by the Herschel-Bulkley three parameter model
- The fluid is incompressible fluid
- There is only laminar flow
- The more viscous fluid is at the bottom called fluid 1 and the less viscous fluid is at he top and is called fluid 2

A Herschel-Bulkley type viscoplasticity with three parameters, i.e., the yield stress, τ_0, the consistency index, m and the shear rate sensitivity index, n, i.e., $\tau_{yz} = \pm\tau_{0i} - m_i\left|\frac{dV^i{}_z}{dy}\right|^{n_i-1}\left(\frac{dV^i{}_z}{dy}\right)$ for $|\tau_{yz}| \geq \tau_0$ (- sign is used for negative shear stress, τ_{yz}, and the shear rate $\left(dV^i{}_z/dy\right)=0$ for $|\tau_{yz}| < \tau_0$ where i represents different zones in the fluids.

There are 12 cases. In the following the details of the derivation of the first case is provided along with the final results for the other 11 cases. The distinguishing features of the 12 cases are also included.

Case I - Details of the Derivation (All Zones)

Condition

$$0 < \lambda_1 < y_i$$

$$y_i \leq \lambda_2, \lambda_3 \leq h$$

Zone 1

$$\frac{d\tau_{yz}{}^1}{dy} = \frac{dp}{dz}$$

on integration, we get

$$\tau_{yz}{}^I = -\frac{dp}{dz}y + c_1^I$$

$$\tau_{yz}{}^{II} = -\frac{dp}{dz} y + c_1^{II}$$

$$\tau_{yz}{}^{III} = -\frac{dp}{dz} y + c_1^{III}$$

$$\tau_{yz}{}^{IV} = -\frac{dp}{dz} y + c_1^{IV}$$

$$\tau_{yz}{}^{V} = -\frac{dp}{dz} y + c_1^{V}$$

From the continuity of shear stress $c_1^I = c_1^{II} = c_1^{III} = c_1^{IV} = c_1^V$, specifying τ_{yz} at one location is adequate at $y = \lambda$, $\tau_{yz} = 0$

$$\therefore \tau_{yz}{}^{i} = -\frac{dp}{dz}(y - \lambda)$$

Case 1 - Diagram (all five zones)

In the previous case

$|\tau_{yz}(0)| > \tau_{0,1}$ at $y = y_i$, $\tau_{yz(1)} = \tau_{yz(2)}$

At $y = \lambda_1$, $|\tau_{yz}| = -\tau_{0,1}$

at $y = \lambda_2$, $|\tau_{yz}| = -\tau_{0,2}$

at $y = \lambda_3$, $|\tau_{yz}| = \tau_{0,2}$

at $y = 0$, $|\tau_{yz}| = \tau_{yz}(0)$

at $y = h$, $|\tau_{yz}| = -\tau_{yz}(h)$

at $\lambda = y = \frac{\lambda_2 + \lambda_3}{2}$, $\tau_{yz} = 0$

Note: $0 < \lambda_1 < y_i$ and $y_i \le \lambda_2, \lambda_3 \le h$

We know that $\tau_{yz} = -\frac{dp}{dz} y + \tau_{yz}(0)$ at $y = \lambda_1, \tau_{yz} = -\tau_{0,1}$. Hence, $\lambda_1 = \left[\frac{-\tau_{0,1} - \tau_{yz}(0)}{(-dp/dz)}\right]$

Note: $\frac{dp}{dz} < 0$

Similarly,

$$\lambda_2 = \left[\frac{-\tau_{0,2} - \tau_{yz}(0)}{(-dp/dz)}\right]$$

$$\lambda_3 = \left[\frac{-\tau_{0,2} - \tau_{yz}(0)}{(-dp/dz)}\right]$$

$$\tau_{yz(h)} = -\frac{dp}{dz} h + \tau_{yz}(0)$$

We need to determine one of these parameters. This can be done by finding the velocity profiles.

1. $V^I_{z,plug} = \beta_1 \left(-\tau_{yz}(0)\right)^{sb_i} + \Lambda_1 \lambda_1^{s_1+1}$ at $y = 0$

2. $V^{II}_z(y_i) = -\Lambda_2 (\lambda_2 - y_i)^{s_2+1} + V^{II}_{z,plug}$ at $y_i \le y < \lambda_2$

$$V^{II}_{z,plug} = \beta_1 \left(-\tau_{yz}(0)\right)^{sb_1} + \Lambda_1 \lambda_1^{s_1} + \Lambda_2 (\lambda_2 - y_i)^{s_2+1}$$

At $y = h$ $\quad V^{II}_z = \beta_2 \left(\tau_{yz}(h)\right)^{sb_2}$

$$V^{II}_{z,plug} = \beta_2 \left(\tau_{yz}(h)\right)^{sb_2} + \Lambda_2 (h - \lambda_3)^{s_2+1}$$

and at $y = \lambda_3$

$$V^{II}_{z,plug} = \beta_1 \left(-\tau_{yz}(0)\right)^{sb_1} + \Lambda_1 \lambda_1^{s_1+1} + \Lambda_2 (\lambda_2 - y_i)^{s_2+1}$$

$\tau_{yz}(0)$ is determined by equating the two previous equations to give

$$\beta_2 \left(\tau_{yz}(h)\right)^{sb_2} + \Lambda_2 (h - \lambda_3)^{s_2+1} = \beta_1 \left(-\tau_{yz}(0)\right)^{sb_1} + \Lambda_1 \lambda_1^{s_1+1} + \Lambda_2 (\lambda_2 - y_i)^{s_2+1}$$

From known $\tau_{yz}(0)$, we determined λ_1, λ_2, and λ_3 from the previous equations.

Zone I

$$0 \le y \le \lambda_1$$

$$V_z^I = \Lambda_1 \left[\lambda_1^{s_1+1} - (\lambda_1 - y)^{s_1+1} \right] - \beta_1 \tau_{yz}(0)$$

Zone II

$$\lambda_1 \le y \le y_i$$

$$V_z^{II} = \Lambda_1 \lambda_1^{s_1+1} - \beta_1 \tau_{yz}(0)$$

Zone III

$$y_i \le y \le \lambda_2$$

$$V_Z^{III} = \Lambda_1 \lambda_1^{s_1+1} - \beta_1 \tau_{yz}(0) + \Lambda_2 \left[(\lambda_2 - y_i)^{s_2+1} - (\lambda_2 - y)^{s_2+1} \right]$$

Zone IV

$$\lambda_2 \le y \le \lambda_3$$

$$V_Z^{IV} = \Lambda_1 \lambda_1^{s_1+1} - \beta_1 \left(\tau_{yz}(0) \right) + \Lambda_2 (\lambda_2 - y_i)^{s_2+1}$$

Zone V

$$\lambda_3 \le y \le h$$

$$V_z^V = \Lambda_1 \lambda_1^{s_1+1} - \beta_1 \tau_{yz}(0) + \Lambda_2 \left[(\lambda_2 - y_i)^{s_2+1} - (y - \lambda_3)^{s_2+1} \right]$$

First determine the plug velocity

Zone II

$$\lambda_1 \le y \le y_i$$

$$V_{z,plug}^1 = \Lambda_1 \lambda_1^{s_1+1} - \beta_1 \left(\tau_{yz}(0) \right)$$

Zone IV

$$\lambda_2 \le y \le \lambda_3$$

$$V_{z,plug}^{II} = V_{z,plug}^1 + \Lambda_2 (\lambda_2 - y_i)^{s_2+1}$$

Zone I

$$0 \le y \le \lambda_1$$

$$V_z^I(y) = V_{z,plug}^I - \Lambda_1(\lambda_1 - y)^{s_1+1}$$

Zone III

$$y_i \le y \le \lambda_2$$

$$V_z^{III}(y) = V_{z,plug}^{II} - \Lambda_2(\lambda_2 - y)^{s_2+1}$$

Zone V

$$\lambda_3 \le y \le h$$

$$V_z^V(y) = V_{z,plug}^{II} - \Lambda_2(y - \lambda_3)^{s_2+1}$$

Modification done for non-linear slip at the wall. The slip velocity at the wall is given by $U_s = \beta\tau_{yz}^{sb}$. Hence, the velocities are as follows

Zone II

$$\lambda_1 \le y \le y_i$$

$$V_{z,plug}^I = \Lambda_1\lambda_1^{s_1+1} - \beta_1\left(\tau_{yz}(0)\right)^{sb_1}$$

Zone IV

$$\lambda_2 \le y \le \lambda_3$$

$$V_{z,plug}^{II} = V_{z,plug}^I + \Lambda_2(\lambda_2 - y_i)^{s_2+1}$$

Zone I

$$0 \le y \le \lambda_1$$

$$V_z^I(y) = V_{z,plug}^I - \Lambda_1(\lambda_1 - y)^{s_1+1}$$

Zone III

$$y_i \le y \le \lambda_2$$

$$V_z^{III}(y) = V_{z,plug}^{II} - \Lambda_2(\lambda_2 - y)^{s_2+1}$$

Zone V

$\lambda_3 \le y \le h$

$$V_z^V(y) = V_{z,plug}^{II} - \Lambda_2 (y - \lambda_3)^{s_2+1}$$

Determination of volumetric flow rate

$$\frac{Q}{W} = \int_0^{\lambda_1} V_z^I dy + \int_{\lambda_1}^{y_i} V_{z,plug}^I dy + \int_{y_i}^{\lambda_2} V_z^{II} dy \int_{\lambda_2}^{\lambda_3} V_{z,plug}^{II} dy \int_{\lambda_3}^{h} V_z^{II} dy$$

On solving we get

$$\frac{Q}{W} = -\Lambda_1 \left[\frac{\lambda_1^{s_1+2}}{s_1+2} - h\lambda_1^{s_1+1} \right] - \Lambda_2 \left[\frac{(\lambda_2 - y_i)^{s_2+2} + (h-\lambda_3)^{s_2+2}}{s_2+2} - (h-y_i)(\lambda_2 - y_i)^{s_2+1} \right] + U_{s,0} h$$

Integration of velocity distribution for volumetric flow rate

Volumetric flow rate of fluid $I = Q^I + Q^{II}$

Volumetric flow rate of fluid $II = Q^{III} + Q^{IV} + Q^V$

$$\frac{Q_{Fluid\ I}}{Q_{Fluid\ II}} = \frac{Q^I + Q^{II}}{\sum_{i=3}^{5} Q^i}$$

$$\frac{Q^I}{W} = V_{z,plug}^I \lambda_1 - \frac{\Lambda_1 \lambda_1^{s_1+2}}{s_1+2}$$

$$\frac{Q^{II}}{W} = V_{z,plug}^I (y_i - \lambda_1)$$

$$\frac{Q^{III}}{W} = V_{z,plug}^{II} (\lambda_2 - y_i) - \frac{\Lambda_2 (\lambda_2 - y_i)^{s_2+2}}{s_2+2}$$

$$\frac{Q^{IV}}{W} = V_{z,plug}^{II} (\lambda_3 - \lambda_2)$$

$$\frac{Q^V}{W} = V_{z,plug}^{II} (h - \lambda_3) - \frac{\Lambda_2 (h-\lambda_3)^{s_2+2}}{s_2+2}$$

$$\frac{Q_{fluid\ 1}}{W} = V^{II}_{z,plug}\, y_i - \frac{\Lambda_1 \lambda_1^{s_1+2}}{s_1+2}$$

$$\frac{Q_{fluid\ 2}}{W} = V^{II}_{z,plug}\,(h-y_i) - \frac{\Lambda_2}{s_2+2}\left[(\lambda_2 - y_i)^{s_2+2} + (h-\lambda_3)^{s_2+2}\right]$$

$$\frac{Q_T}{W} = V^{I}_{z,plug}\, y_i - \frac{\Lambda_1 \lambda_1^{s_1+2}}{s_1+2} + V^{II}_{z,plug}\,(h-y_i) - \frac{\Lambda_2}{s_2+2}\left[(\lambda_2 - y_i)^{s_2+2} + (h-\lambda_3)^{s_2+2}\right]$$

Case II (no zone 2)

The details of the derivation are not provided, but are similar to case I, which were given previously.

Condition

$$y_i \le \lambda_1$$

$$y_i \le \lambda_2$$

$$\lambda_3 \le h$$

Zone I

$$0 \le y \le y_i$$

$$V_z^I(y) = V^{II}_{z,plug} - \Lambda_2(\lambda_2 - y_i)^{s_2+1} - \Lambda_1\left[(\lambda_1 - y)^{s_1+1} - (\lambda_1 - y_i)^{s_1+1}\right]$$

Zone IV

$$\lambda_2 \le y \le \lambda_3$$

$$V^{II}_{z,plug} = \beta_2\left(\tau_{yz}(h)\right)^{sb_2} + \Lambda_2(h-\lambda_3)^{s_2+1}$$

Zone III

$$y_i \le y \le \lambda_2$$

$$V_z^{III}(y) = V^{II}_{z,plug} - \Lambda_2(\lambda_2 - y)^{s_2+1}$$

Zone V

$$V_z^V(y) = \beta_2\left(\tau_{yz}(h)\right)^{sb_2} + \Lambda_2\left[(h-\lambda_3)^{s_2+1} - (y-\lambda_3)^{s_2+1}\right]$$

Overall flow rate

$$\frac{Q_T}{W} = \Lambda_2\left[-(\lambda_2 - y_i)^{s_2+1}(y_i) - \frac{(\lambda_2 - y_i)^{s_2+2}}{s_2+2} + h(h-\lambda_3)^{s_2+2} - \frac{(h-\lambda_3)^{s_2+2}}{s_2+2}\right]$$

$$+\Lambda_1\left[\frac{(\lambda_1 - y_i)^{s_1+2} - \lambda_1^{s_1+2}}{s_1+2} + y_i(\lambda_1 - y_i)^{s_1+1}\right] + h\beta_2\left(\tau_{yz}(h)\right)^{sb_2}$$

Case III (no zone I)

Condition

$y_i \le \lambda_2$

$\lambda_3 \le h$

$\lambda_1 < 0$

Determination of $\tau_{yz}(0)$

$$\beta_2\left(\tau_{yz}(h)\right)^{sb_2} + \Lambda_2(h-\lambda_3)^{s_2+1} = \beta_1\left(-\tau_{yz}(0)\right)^{sb_1} + \Lambda_2(\lambda_2 - y_i)^{s_2+1}$$

Zone II

$0 \le y \le y_i$

$$V_{z,plug}^{1} = \beta_1\left(\tau_{yz}(0)\right)^{sb_1}$$

Zone III

$y_i \le y \le \lambda_2$

$$V_z^{II}(y) = \beta_1\left(-\tau_{yz}(0)\right)^{sb} + \Lambda_2\left[(\lambda_2 - y_i)^{s_2+1} - (\lambda_2 - y)^{s_2+1}\right]$$

Zone IV

$\lambda_2 \le y \le \lambda_3$

$$y = \lambda_2, V_z^{IV} = V_{z,plug}^{II} = \beta_1\left(\tau_{yz}(0)\right)^{sb_1} + \Lambda_2(\lambda_2 - y_i)^{s_2+1}$$

Zone V

$$\lambda_3 \le y \le h$$

$$V_z^V(y) = V_{z,plug}^{II} - \Lambda_2 (y - \lambda_3)^{s_2+1}$$

Overall flow rate

$$\frac{Q_T}{W} = \Lambda_2 \left[\frac{(\lambda_2 - y_i)^{s_2+2} + (h - \lambda_3)^{s_2+2}}{s_2 + 2} - (\lambda_2 - y_i)^{s_2+1}(h - y_i) \right] + h\beta_1 \left(-\tau_{yz}(0)\right)$$

Case IV (no zone 3)

Condition

$$0 \le \lambda_1 \le y_i$$

$$y_i \le \lambda_2 \le hs$$

$$\lambda_2 \le y_i$$

Determination of $\tau_{yz}(0)$

$$\beta_2 \left(\tau_{yz}(h)\right)^{sb_2} + \Lambda_2 (h - \lambda_3)^{s_2+1} = \beta_1 \left(-\tau_{yz}(0)\right)^{sb_1} + \Lambda_1 (\lambda_1)^{s_1+1}$$

Zone I

$$0 \le y \le \lambda_1$$

$$V_z^I(y) = V_{z,plug}^I - \Lambda_1 (\lambda_1 - y)^{s_1+1}$$

Zone II

$$\lambda_1 \le y \le y_i$$

$$V_{z,plug}^I = \Lambda_1 \lambda_1^{s_1+1} - \beta_1 \tau_{yz}(0)$$

Zone IV

At $y = y_i$

$$V_{z,plug}^{II} = V_{z,plug}^I$$

At $y_i \le y \le \lambda_3$

$$V_z^{IV} = V_{z,plug}^{II} = \beta_1\left(-\tau_{yz}(0)\right)^{sb_1} + \Lambda_1\lambda_1^{s_1+1}$$

Zone V

$$\lambda_3 \le y \le h$$

$$V_z^{V}(y) = V_{z,plug}^{II} - \Lambda_2(y-\lambda_3)^{s_2+1}$$

Overall flow rate

$$\frac{Q_T}{W} = \left[\beta_1\left(-\tau_{yz}(0)\right)^{sb_1} + \Lambda_1\lambda_1^{s_1+1}\right]h - \Lambda_1\frac{\lambda_1^{s_2+2}}{s_1+2} - \Lambda_2\left[\frac{(h-\lambda_3)^{s_2+2}}{s_2+2}\right]$$

Case V (no zones 1 or 3)

Condition

$$y_i \le \lambda_3 \le h$$

$$\lambda_2 \le y_i$$

$$\lambda_1 \le 0$$

Determination of $\tau_{yz}(0)$

$$\beta_2\left(\tau_{yz}(h)\right)^{sb_2} + \Lambda_2(h-\lambda_3)^{s_2+1} = \left[-\beta_1\tau_{yz}(0)\right]^{sb_1}$$

Zone II

$$0 \le y \le y_i$$

$$V_z^{II} = V_{z,plug}^{II} = V_{z,plug}^{1} = \left[-\beta_1\tau_{yz}(0)\right]^{sb_1}$$

Zone IV

$$y_i \le y \le \lambda_3$$

$$V_z^{IV} = V_{z,plug}^{II} = V_{z,plug}^{I} = \left[-\beta_1\tau_{yz}(0)\right]^{sb_1}$$

Zone V

At $y = \lambda_3$

$$V_z^V = V_{z,plug}^{II}$$

At $y = h$

$$V_z^V = \beta_2 \left(\tau_{yz}(h)\right)^{sb_2}$$

Overall flow rate

$$\frac{Q_T}{W} = \left[\beta_1 \left(-\tau_{yz}(0)\right)^{sb_1}\right] h - \Lambda_2 \left[\frac{(h-\lambda_3)^{s_2+2}}{s_2+2}\right]$$

Case VI (no zones 1, 3, or 5)

Condition

$$\lambda_1 \le 0$$

$$\lambda_2 \le y_i$$

$$\lambda_3 \ge h$$

Determination of $\tau_{yz}(0)$

$$\beta_2 \left(\tau_{uz}(0) - \frac{dp}{dz} h\right)^{sb_2} = \beta_1 \left(-\tau_{yz}(0)\right)^{sb_1}$$

Zone II

$$0 \le y \le y_i$$

$$V_z^{II}(y) = \beta_1 \left(-\tau_{yz}(0)\right)^{sb_1}$$

Zone IV

At $y = y_i$

$$V_{z,plug}^{II} = V_{z,plug}^{I}$$

At $y_i \le y \le h$

$$V_z^{IV} = V_{z,plug}^{II} = \beta_2 \left(-\tau_{yz}(0)\right)^{sb_2}$$

Overall flow rate

$$\frac{Q_T}{W} = \left[\beta_1 \left(-\tau_{yz}(0)\right)^{sb_1}\right] h$$

Case VII (no zone 5)

Condition

$$0 \le \lambda_1 \le y_i$$

$$y_i \le \lambda_2 \le h$$

$$\lambda_3 \ge h$$

Zone I

$$0 \le y \le \lambda_1$$

$$V_z^I = \Lambda_1 \left[\lambda_1^{s_1+1} - (\lambda_1 - y)^{s_1+1}\right] - \beta_1 \left(\tau_{yz}(0)\right)^{sb_1}$$

Zone II

$$\lambda_1 \le y \le y_i$$

$$V_z^{II} = V_{z,plug}^I = -\beta_1 \left(\tau_{yz}(0)\right)^{sb_1} + \Lambda_1 \lambda_1^{s_1+1}$$

Zone III

$$y_i \le y \le \lambda_2$$

$$V_z^{III} = \Lambda_1 \lambda_1^{s_1+1} - \beta_1 \left(\tau_{yz}(0)\right)^{sb_1} + \Lambda_2 \left[(\lambda_2 - y_i)^{s_2+1} - (\lambda_2 - y)^{s_2+1}\right]$$

Zone IV

$$\lambda_2 \le y \le \lambda_3$$

$$V_z^{IV} = \Lambda_1 \lambda_1^{s_1+1} - \beta_1 \left(\tau_{yz}(0)\right)^{sb_1} + \Lambda_2 (\lambda_2 - y_i)^{s_2+1}$$

Determination of $\tau_{yz}(0)$

$$V_{z,plug}^{II} = \beta_2\left(\pm\tau_{yz}(h)\right)^{sb_2} = V_{z,plug}^{II}$$

Overall flow rate

$$\frac{Q_T}{W} = \Lambda_2\left[(\lambda_2 - y_i)^{s_2+1}(h - y_i) - \frac{(\lambda_2 - y_i)^{s_2+2}}{s_2+2}\right] - \beta_1\left(-\tau_{yz}(0)\right)^{sb_1} h + \Lambda_1\left[h\lambda_1^{s_1+1} - \frac{\lambda_1^{s_1+2}}{s_1+2}\right]$$

Case VIII (no zone 2 or 5)

Condition

$$\lambda_1 > y_i$$

$$y_i \le \lambda_2 \le h$$

$$\lambda_3 \ge h$$

Zone I

$$0 \le y \le y_i$$

$$V_z^I = \beta_1\left(\tau_{yz}(0)\right)^{sb_1} + \Lambda_1\left[\lambda_1^{s_1+1} - (\lambda_1 - y)^{s_1+1}\right]$$

Zone III

$$y_i \le y \le \lambda_2$$

$$V_z^{III} = \beta_1\left(\tau_{yz}(0)\right)^{sb_1} + \Lambda_1\left[(\lambda_1)^{s_1+1} - (\lambda_1 - y_i)^{s_1+1}\right] + \Lambda_2\left[(\lambda_2 - y_i)^{s_2+1} - (\lambda_2 - y)^{s_2+1}\right]$$

Zone IV

$$\lambda_2 \le y \le h$$

$$V_z^{IV} = \beta_2\left(\tau_{yz}(0)\right)^{sb_2} - \Lambda_2(\lambda_2 - y)^{s_2+1}$$

Determination of $\tau_{yz}(0)$

$$V_{z,plug}^{II} = \beta_2\left(\pm\tau_{yz}(h)\right)^{sb_2} = V_{z,plug}^{II}$$

Overall flow rate

$$\frac{Q_T}{W} = \Lambda_2\left[\frac{(\lambda_2 - y_i)^{s_1+2}}{s_2+2}\right] + \beta_1\left(-\tau_{yz}(0)\right)^{sb_2} y_i + \Lambda_1\left[\frac{(\lambda_1 - y_i)^{s_1+2} - \lambda_1^{s_1+2}}{s_1+2}\right] + \beta_2\left(\pm\tau_{yz}(h)\right)^{sb_2}(h - y_i)$$

Case IX (no zones 1 or 5)

Condition

$$\lambda_1 < 0$$

$$y_i \le \lambda_2$$

$$\lambda_3 \le h$$

Zone II

$$0 \le y \le y_i$$

$$V_{z,plug}^{I} = \beta_1\left(-\tau_{yz}(0)\right)^{sb_1}$$

Zone III

$$V_z^{II}(y) = \beta_1\left(-\tau_{yz}(0)\right)^{sb_1} + \Lambda_2\left[(\lambda_2 - y_i)^{s_2 1} - (\lambda_2 - y)^{s_2+1}\right]$$

Zone IV

$$\lambda_2 \le y \le h$$

$$Aty = \lambda_2, V_z^{IV} = V_{z,plug}^{II} = \Lambda_2(\lambda_2 - y_i)^{s_2+1} - \beta_1\left(\tau_{yz}(0)\right)^{sb_1}$$

Determination of $\tau_{yz}(0)$

$$\beta_2\left(\pm\tau_{yz}(h)\right)^{sb_2} = \beta_1\left(-\tau_{yz}(0)\right)^{sb_1} + \Lambda_2(\lambda_2 - y_i)^{s_2+1}$$

Overall flow rate

$$\frac{Q_T}{W} = \beta_1\left(-\tau_{yz}(0)\right)^{sb_1}(y_i) - \Lambda_2\left[\frac{(\lambda_2 - y_i)^{s_2+2}}{s_2+2}\right] + \beta_2\left(\pm\tau_{yz}(h)\right)^{sb_2}(h - y_i)$$

Case X (no zones 2 or 3)

Condition

$$y_i \le \lambda_1$$

$$y_i \ge \lambda_2$$

$$y_i \le \lambda_3 \le h$$

Zone I

$$0 \le y \le y_i \lambda_2 < y_i$$

$$V_z^I = \beta_1 \left(-\tau_{yz}(0)\right)^{sb_1} - \Lambda_1 \left\lfloor (\lambda_1 - y)^{s_1+1} - \lambda_1^{s_1+1} \right\rfloor$$

Zone IV

$$y_i \le y \le \lambda_3$$

$$V_z^{IV} = \Lambda_2 \left\lfloor (h-\lambda_3)^{s_2+1} - -(y-\lambda_3)^{s_2+1} \right\rfloor + \beta_2 \left(\tau_{yz}(h)\right)^{sb_2}$$

Zone V

$$\lambda_3 \le y \le h$$

$$V_z^V = \beta_2 \left(\tau_{yz}(h)\right)^{sb_2} + \Lambda_2 \left\lfloor (h-\lambda_3)^{s_1+1} - (y-\lambda_3)^{s_2+1} \right\rfloor$$

Determination of $\tau_{yz}(0)$

$$\beta_1 \left(-\tau_{yz}(0)\right)^{sb_1} - \Lambda_1 \left\lfloor (\lambda_1 - y_i)^{s_1+1} - \lambda_1^{s_1+1} \right\rfloor = \beta_2 \left(\tau_{yz}(h)\right)^{sb_2} + \Lambda_2 \left\lfloor (h-\lambda_3)^{s_2+1} \right\rfloor$$

Overall flow rate

$$\frac{Q_T}{W} = \Lambda_2 \left[(h-\lambda_3)^{s_2+1}(h-y_i) - \frac{(h-\lambda_3)^{s_2+2}}{(s_2+2)} \right] + \beta_1 \left(-\tau_{yz}(0)\right)^{sb_2} y_i + \Lambda_1 \left[\frac{(\lambda_1 - y_i)^{s_1+2} - \lambda_1^{s_1+2}}{s_1+2} + \lambda_1^{s_1+1} y_i \right]$$

Case XI (no zones 2, 3, or 5)

Condition

$$y_i \le \lambda_i$$

$$\lambda_3 > h$$

$$\lambda_2 < y_i$$

Zone 1

$$0 \le y \le y_i;\ \lambda_2 < y_i$$

$$V_z^I = \beta_1\left(-\tau_{yz}(0)\right)^{sb_1} - \Lambda_1\left[(\lambda_1 - y)^{s_1+1} - \lambda_1^{s_1+1}\right]$$

Zone IV

$$y_i \le y \le \lambda_3$$

$$\lambda_3 > h$$

$$\lambda_2 < y_i$$

$$V_z^{IV} = \beta_2\left(\tau_{yz}(h)\right)^{sb_2}$$

Determination of $\tau_{yz}(0)$

$$\beta_1\left(-\tau_{yz}(0)\right)^{sb_1} - \Lambda_1\left[(\lambda_1 - y_i)^{s_1+1} - \lambda_1^{s_1+1}\right] = \beta_2\left(\tau_{yz}(h)\right)^{sb_2}$$

Overall flow rate

$$\frac{Q_T}{W} = \beta_1\left(-\tau_{yz}(0)\right)^{sb_1} y_i + \Lambda_1\left[\frac{(\lambda_1 - y_i)^{s_1+2} - \lambda_1^{s_1+2}}{s_1+2}\right] + \beta_2\left(\pm\tau_{yz}(h)\right)^{sb_2}(h - y_i) + \lambda_1^{s_1+1} y_i$$

Case XII (no zones 3 or 5)

Condition

$$0 \le \lambda_1 \le y_i$$

$$\lambda_3 > h$$

$$\lambda_2 < y_i$$

Zone 1

$$0 \le y \le \lambda_1$$

$$V_z^I = -\Lambda_1 \left[(\lambda_1 - y)^{s_1+1} - \lambda_1^{s_1+1} \right] + \beta_1 \left(-\tau_{yz}(0) \right)^{sb_1}$$

Zone II

$$\lambda_1 \le y \le y_i$$

$$V_z^{II} = V_{z,plug}^I = \beta_1 \left(-\tau_{yz}(0) \right)^{sb_1} + \Lambda_1 \lambda_1^{s_1+1}$$

Zone IV

$$V_z^{II} = V_{z,plug}^{II} = \Lambda_1 \lambda_1^{s_1+1} - \beta_1 \left(\tau_{yz}(0) \right)^{sb_1}$$

Determination of $\tau_{yz}(0)$

$$V_{z,plug}^I = \beta_1 \left(-\tau_{yz}(0) \right)^{sb_1} + \Lambda_1 \lambda_1^{s_1+1} = \beta_2 \left(\tau_{yz}(h) \right)^{sb_2} = V_{z,plug}^{II}$$

Overall flow rate

$$\frac{Q_T}{W} = h\beta_2 \left(\pm \tau_{yz}(h) \right)^{sb_2} - \Lambda_1 \left[\frac{\lambda_1^{s_1} 2}{s_1 + 2} \right]$$

Conditions to determine which case applies

Case I (all zones)

$$0 < \lambda_1 < y_i, \; y_i \le \lambda_2, \; \lambda_3 \le h$$

Case II (no zone 2)

$$y_i \le \lambda_1, \; y_i \le \lambda_2, \; \lambda_3 \le h$$

Case III (no zone 1)

$$y_i \le \lambda_2, \; \lambda_3 \le h, \; \lambda_1 < 0$$

Case IV (no zone 3)

$$0 \le \lambda_1 \le y_i, \; y_i \le \lambda_2 \le h, \; \lambda_2 \le y_i$$

Case V (no zone 1 or 3)

$$y_i \le \lambda_3 \le h,\ \lambda_2 \le y_i,\ \lambda_1 \le 0$$

Case VI (no zone 1, 3, or 5)

$$\lambda_1 \le 0,\ \lambda_2 \le y_i,\ \lambda_3 \ge h$$

Case VII (no zone 5)

$$0 \le \lambda_1 \le y_i,\ y_i \le \lambda_2 \le h,\ \lambda_3 \ge h$$

Case VIII (no zone 2 or 5)

$$\lambda_1 > y_i,\ y_i \le \lambda_2 \le h,\ \lambda_3 \ge h$$

Case IX (no zone 1 or 5)

$$\lambda_1 < 0,\ y_i \le \lambda_2,\ \lambda_3 \le h$$

Case X (no zones 2 or 3)

$$y_i \le \lambda_1,\ y_i \ge \lambda_2,\ y_i \le \lambda_3 \le h$$

Case XI (no zones 2, 3, or 5)

$$y_i \le \lambda_i,\ \lambda_3 > h,\ \lambda_2 < y_i$$

Case XII (no zones 3 or 5)

$$0 \le \lambda_1 \le y_i,\ \lambda_3 > h,\ \lambda_2 < y_i$$

Typical comparisons of the experimental results versus the predictions of the model are shown in figures 31 to 34. Overall, the predictions of the flow rate versus the pressure drop are adequate.

SUMMARY OF GENERAL CONCLUSIONS AND LESSONS

- The manufacturing of co-extruded grains of highly filled propellants is an intricate process, which requires a realistic understanding of the various types of interface, surface and bulk instabilities.

- The interface between the two fluids can shift during the co-extrusion process if the wall slip and the shear viscosity of the two phases are not similar.

- One or both of the two surfaces of the co-extruded grains can be subjected to flow instabilities and the related development of gross surface irregularities, which can render the products unacceptable.

- The use of mathematical modeling allows the understanding of the details of the process to make educated designs and selection of processing conditions possible, however, these models need to be further expanded, validated and converted into tools that are user-friendly for the day to day workings of the Department of Defense.

Specific Conclusions and Lessons

Material Characterization

- Consistent with what we have advocated since 1986, the wall-slip behavior and the viscoplasticity of the phases to be co-extruded need to be accurately determined. It is now clear that the platform that we have established is equally valid for the co-extrusion process.

- The critical shear stress at which the transition from stick to slip for a given suspension should be an additional parameter to be characterized during the characterization of the phases.

- The compressibility of the melt/suspension and the pressure dependence of the slip coefficients need to be incorporated into the mathematical models of the co-extrusion process to accurately determine the conditions under which flow instabilities are on-set, so that such instabilities can be minimized or eliminated.

Formulation for Processability

- The formulations of the two phases to be co-extruded should be tailored if possible to match the wall slip behavior and the shear viscosities of the two phases to be co-extruded.

- If the differences in the rheological behavior of the two phases are not significant then the interface remains stable during the co-extrusion flow.

- If the wall-slip condition remains stable during processing flow instabilities are not encountered and the formulation affects the stability of the wall slip condition also.

Mathematical Modeling

- We have derived a complete set of equations to describe the co-extrusion of viscoplastic fluids subject to wall slip in various configurations, including the side by side co-extrusion of two viscoplastic fluids, a case studied extensively with our experimental setup.

- The comparisons of the results of the experimental studies with the mathematical modeling results is acceptable at moderate rates, however, problems are noted at the low and high flow rate regions.

- The sources of the discrepancies for co-extrusion at the low and high flow rates need to be determined, especially by revisiting the fits of the wall slip and shear viscosity characterizations at the low and high shear rates (parameters generally do not cover the entire range of shear rates).

- We have developed a new model to predict the on-set of flow instabilities on the basis of the compressibility of the melt/suspension and the change in the wall slip coefficient with pressure along the length of the die, which appears to be very accurate for extrusion flows.

- However, the compressible fluid model needs to be expanded into the co-extrusion process.

- At the first opportunity possible, the steady FEM models of SIT will need to be converted into time dependent models to allow time dependent calculations to be made for process control purposes (model based process control) and better design of the process. Such calculations can also be used to generate functionally graded co-extruded propellants in the axial direction in a cyclic fashion.

Design and Operating Condition Selections

- If the formulations cannot be tailored to match the rheological behavior then the geometries and operating conditions should be tailored to allow the ultimate rheological behavior of the two phases in the co-extrusion die to match. This can be accomplished to some extent, for example, by the selection of two different temperatures for the two phases.

- It is the presence of the converging section in the design that we have selected which has given rise to the changing interface location as a function of time during co-extrusion. More of PDMS has flown in the die and thus more of it is depleted from the reservoir section during the course of the co-extrusion followed by the depletion of the pure PDMS and then the consequent increase in the flow rate of the filled PDMS which now occupies more of the converging section of the die.

- A reservoir region adjacent to the fully developed section of the die should never be included in the design of the co-extrusion die.

- One needs to determine apriori flow conditions, which provide extrudates that are free of surface irregularities on their entire perimeter.

On-line Process and Product Quality Control

- The pressure readings change very little during the process, however, the change in the pressure gradient is significant along with a significant change in the interface location.

- Thus, during the co-extrusion process one either needs to determine the pressure values very accurately to generate accurate pressure gradient values and/or continuously follow the interface location as a function of time during the co-extrusion process.

- Currently, there is no method to follow on an on-line basis the interface location during co-extrusion. This problem needs to be addressed as a quality control issue.

- If the temperature distributions of the two streams change as a function of time during the co-extrusion process the interface location is likely to change also, since the shear viscosity and wall slip will also change. Thus, the operating conditions need to be carefully selected and then maintained during the process.

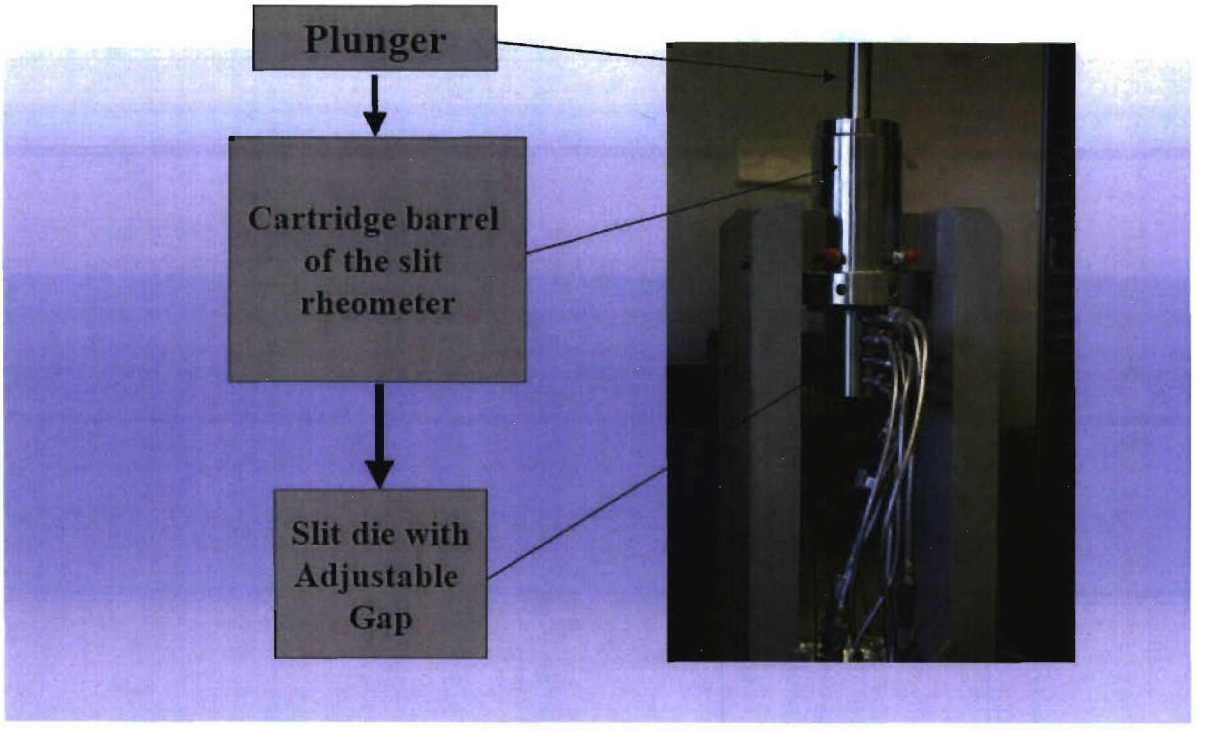

Figure 1
Principal experimental arrangement for approaching the co-extrusion problem; off-line slit rheometer

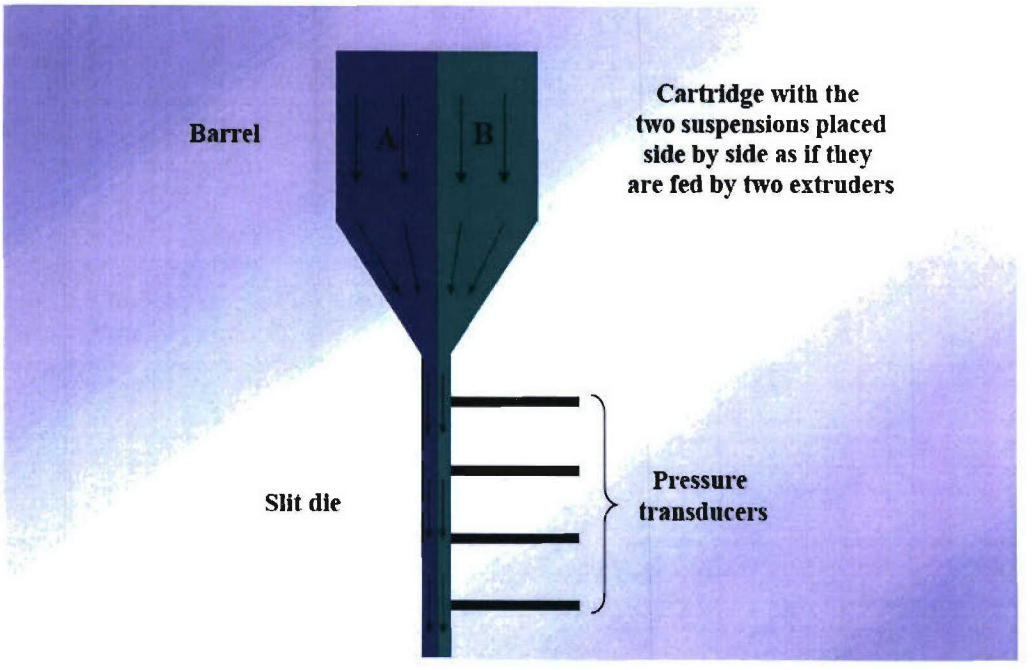

Figure 2
Apparatus for the investigation of the shape of the interface and flow/interface instabilities

Figure 3
Placement of a partition in the mid-plane of the cartridge and the two sides for allowing the interface to be traced

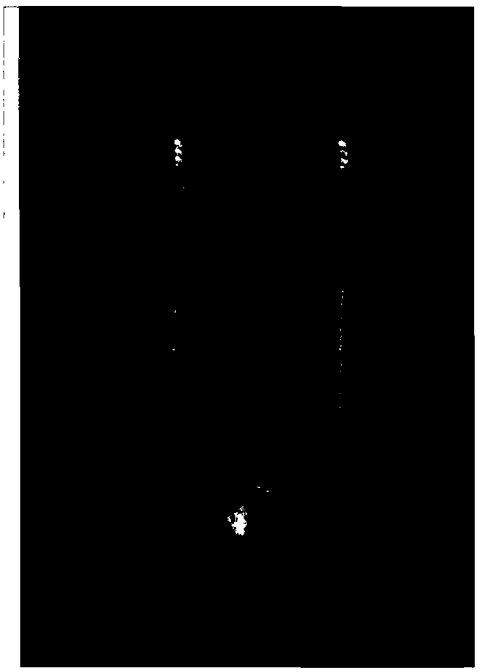

Figure 4
Partition and cartridge used in the experiments

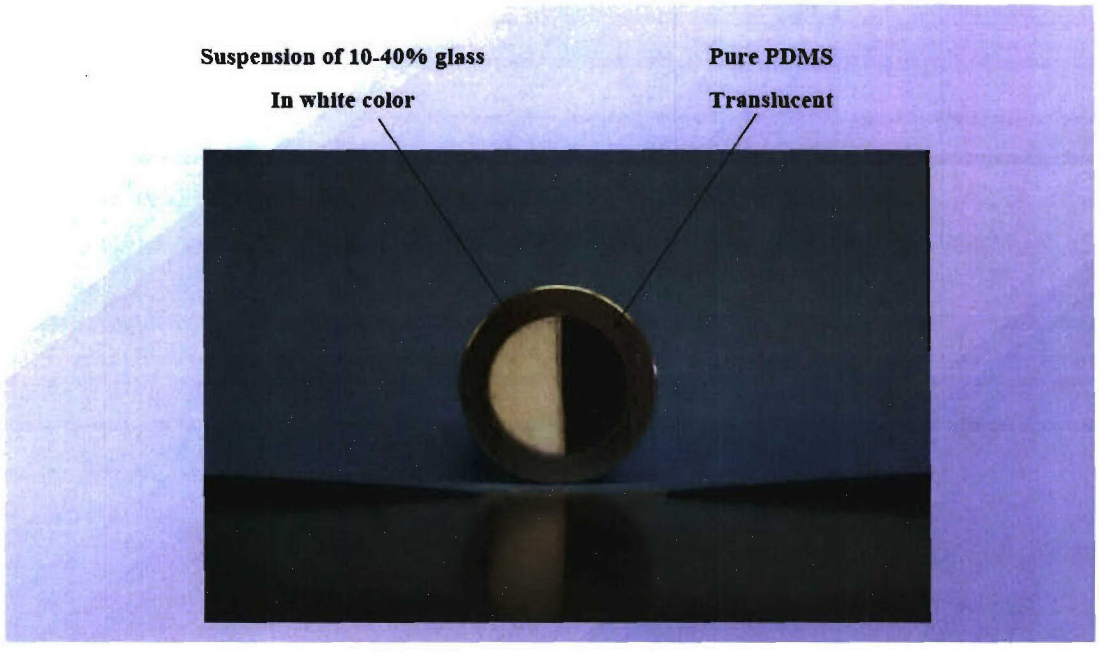

Figure 5
Coloring of the two different co-extrusion layers

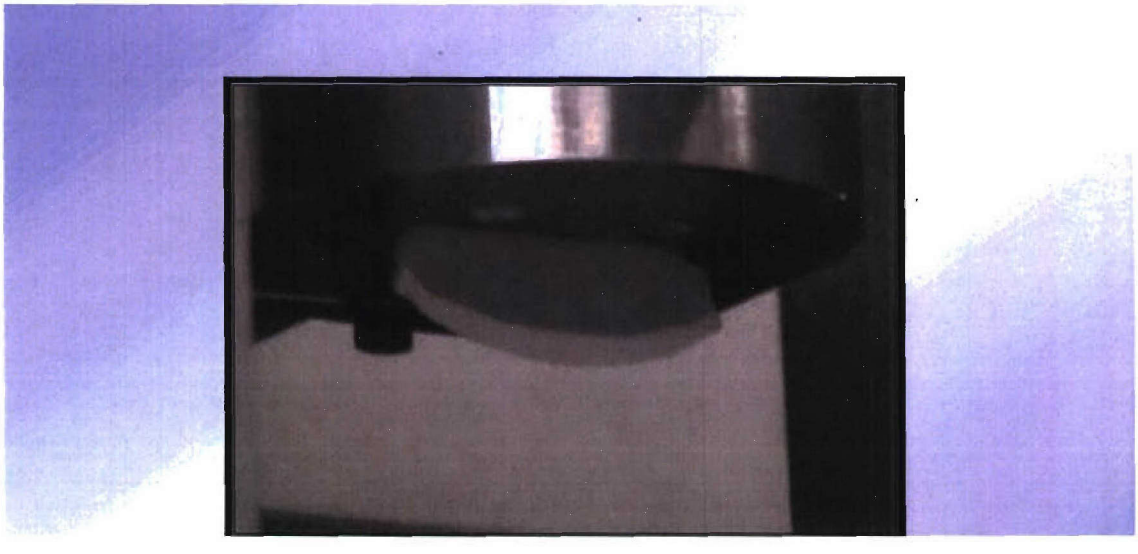

Figure 6
Exit of the co-extruded grain from the slit die

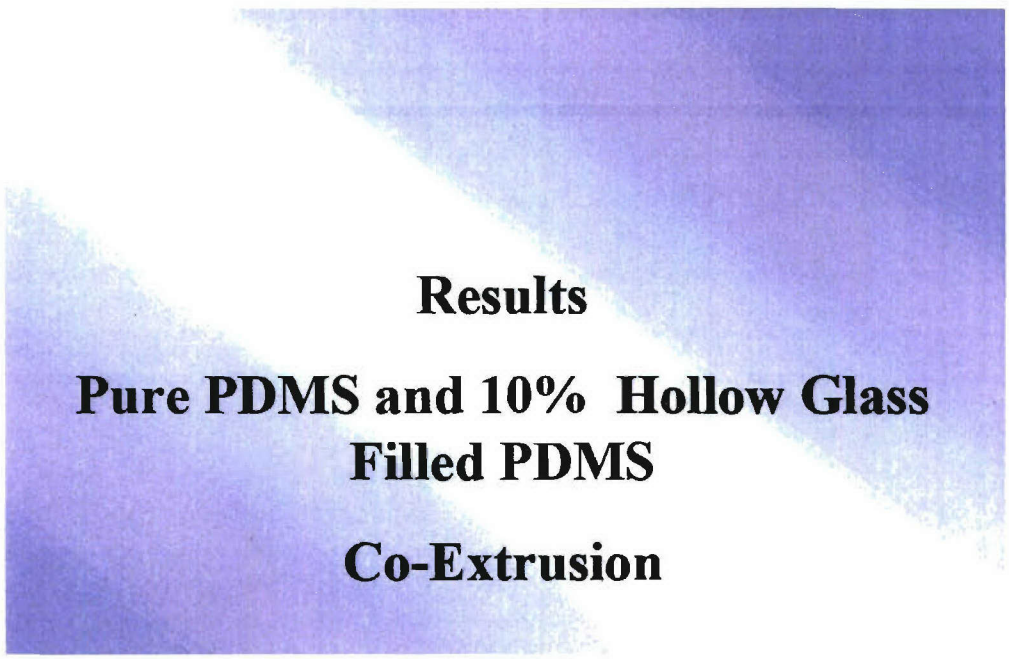

Figure 7
Results for 0 and 10% co-extrusion

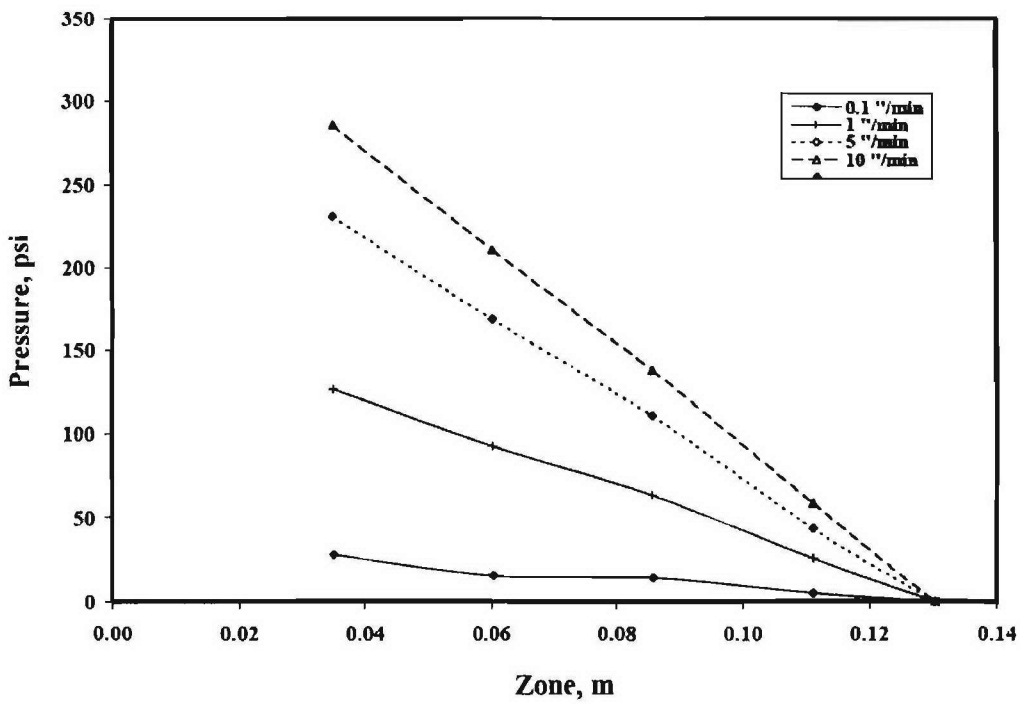

Figure 8
Pressure versus distance in the slit die for different flow rates (cross-head speeds)

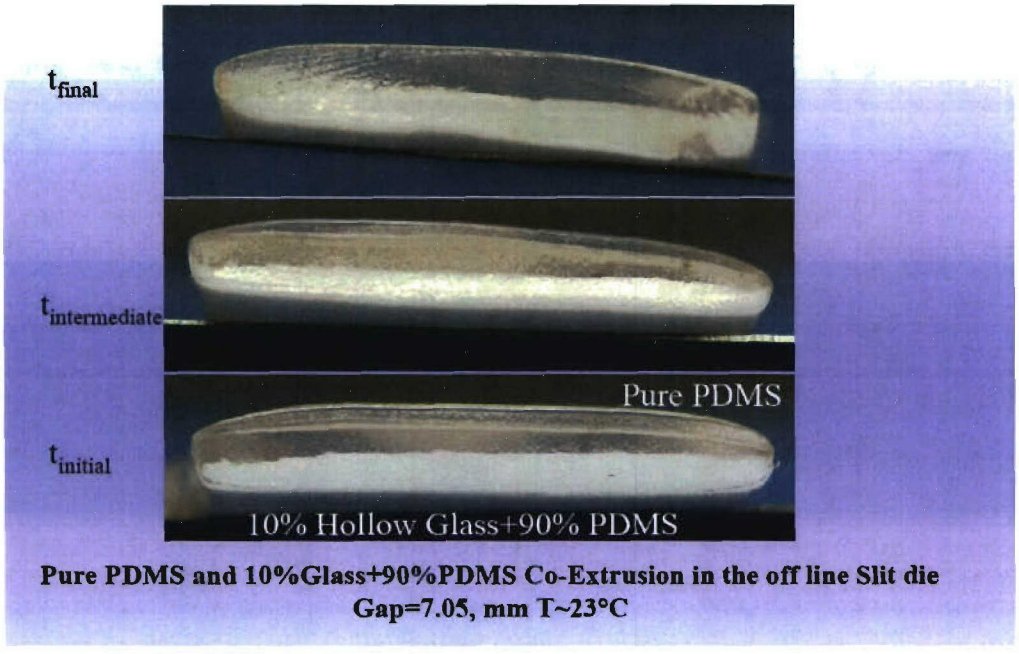

Figure 9
Distribution of the two-co-extruded layers during extrusion: 0.1 in./min, cut in the transverse to flow direction

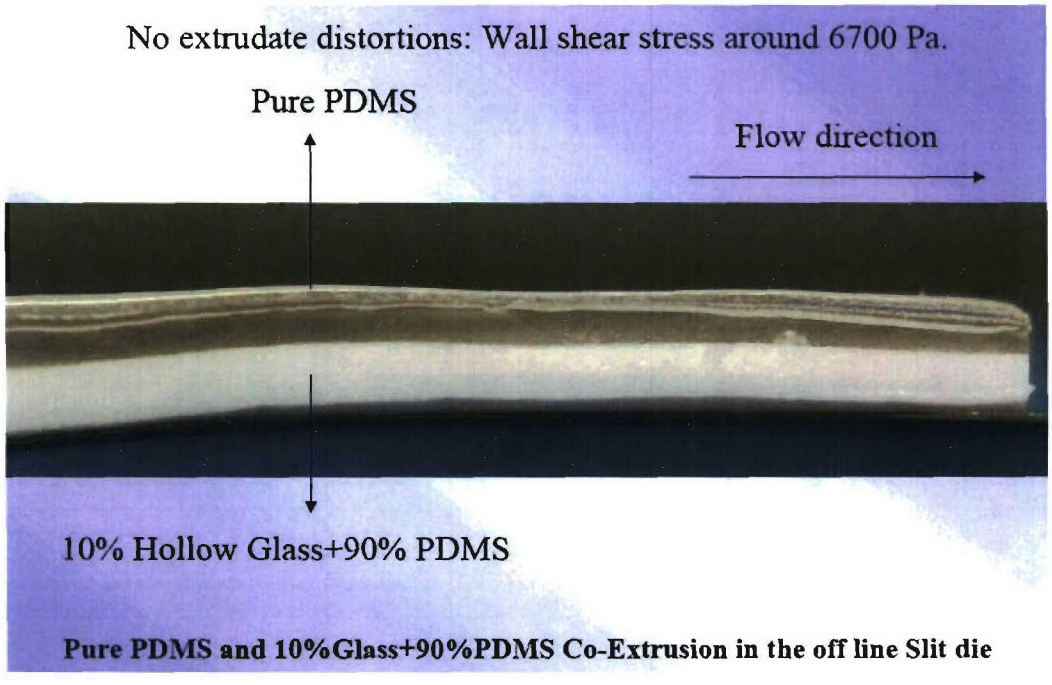

Figure 10
Distribution of the two co-extruded layers during extrusion: 0.1 in./min, cut in the transverse to flow direction

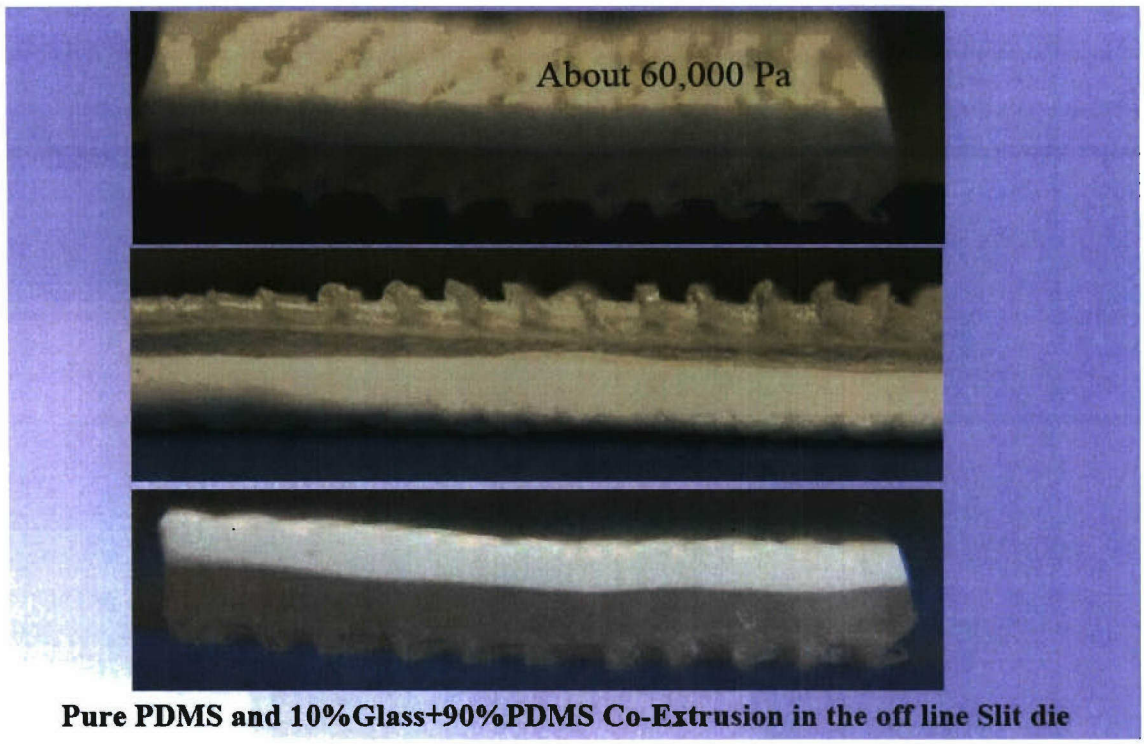

Figure 11
Distribution of the two co-extruded layers during extrusion: 0.1 in./min, cut in the parallel to flow direction

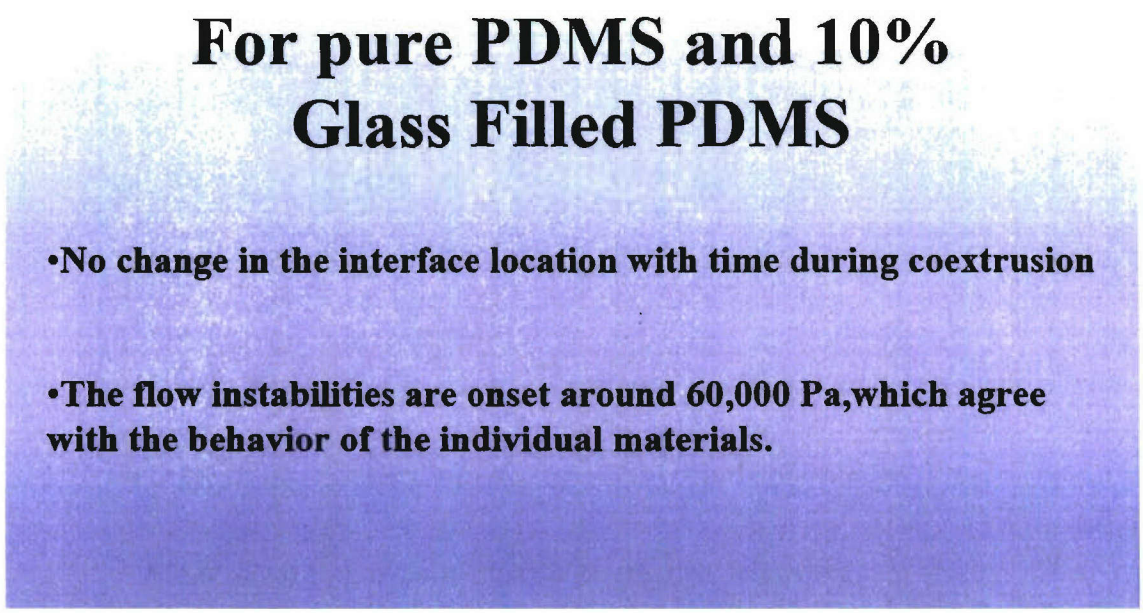

Figure 12
Summary of co-extrusion results for pure PDMS and 10% by volume glass

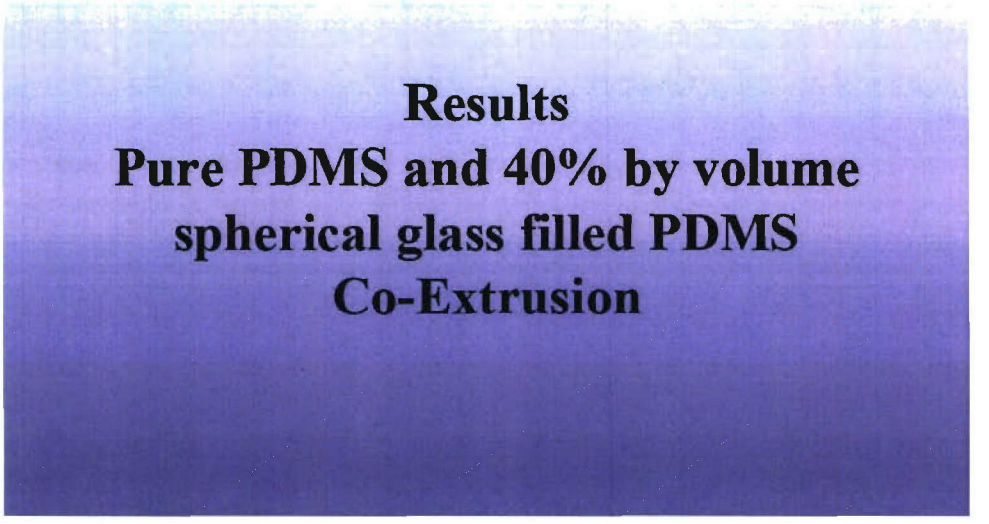

Figure 13
Results for 0 and 40%

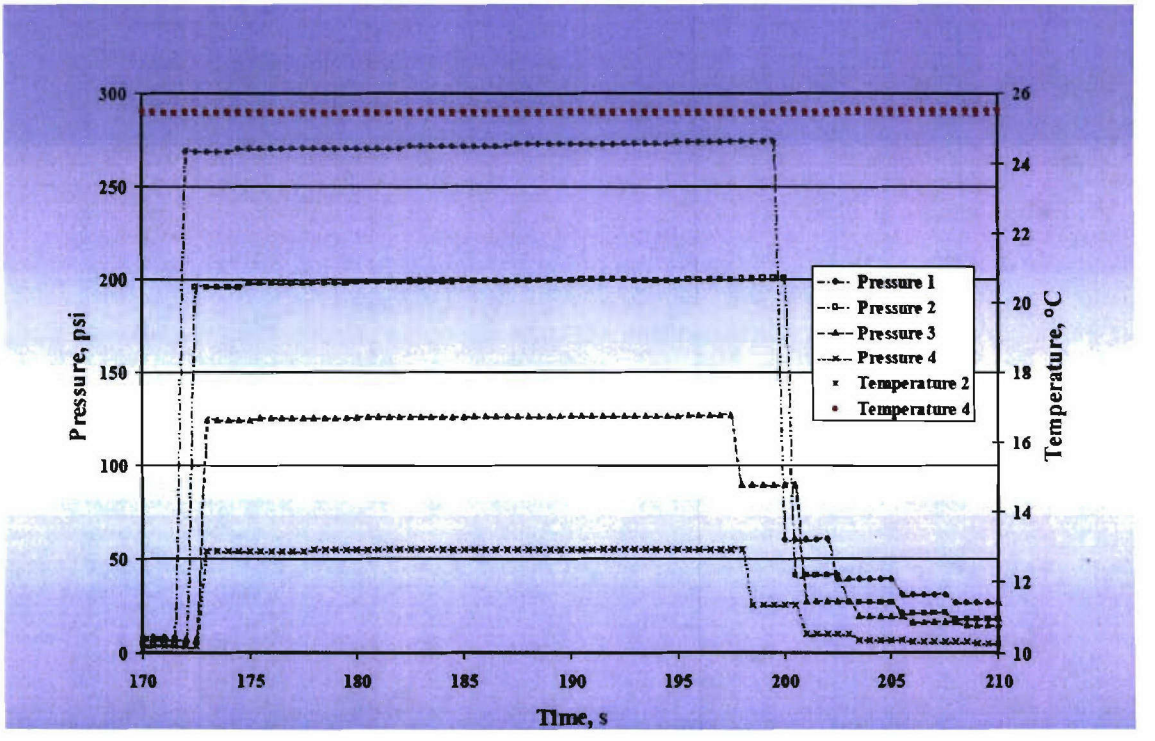

Figure 14
Pressure versus time for co-extrusion of 0 and 40%

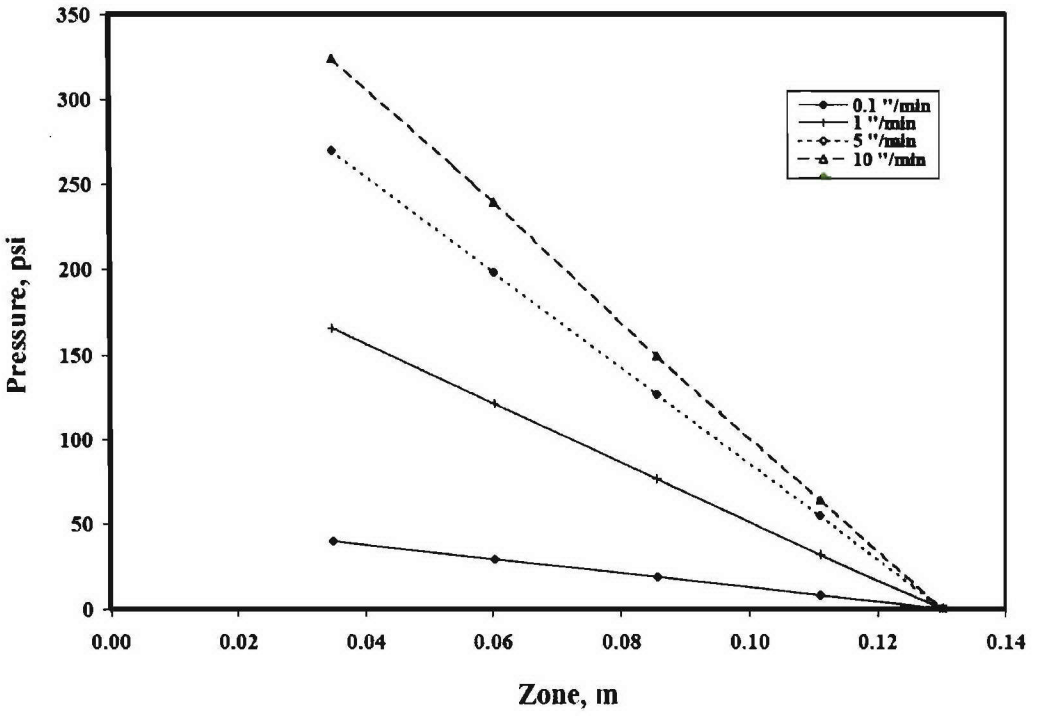

Figure 15
Pressure versus distance in the slit die for different flow rates (cross-head speeds) during co-extrusion of 0 and 40%

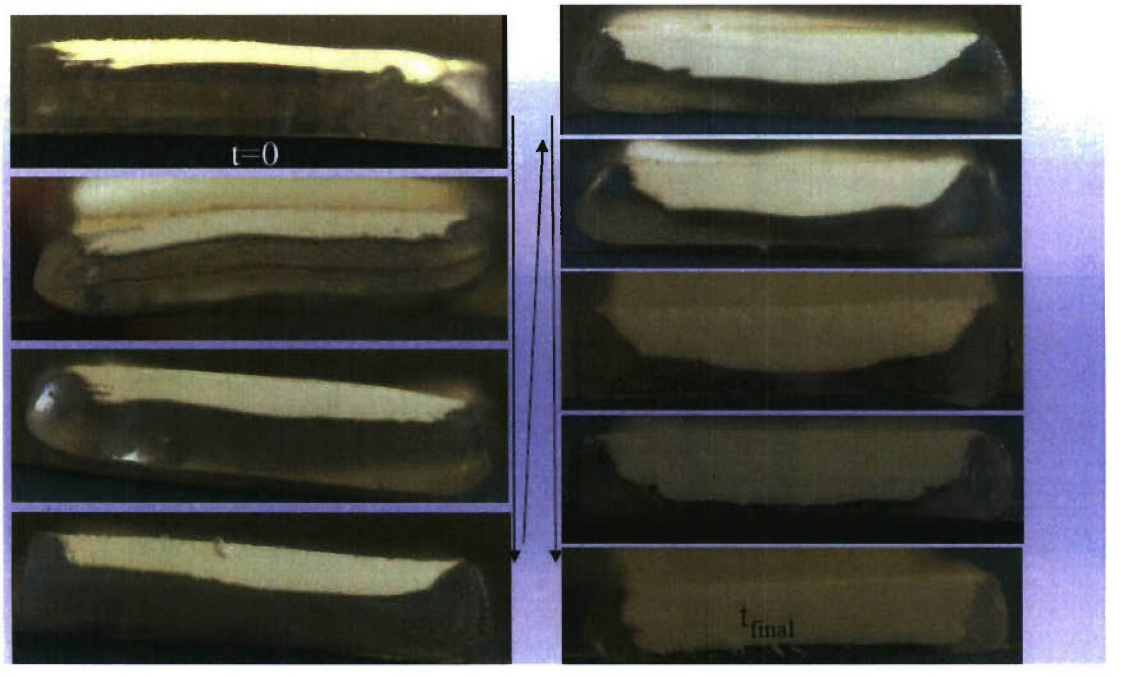

Figure 16
Distribution of the two co-extruded layers during extrusion: 0.1 in./min, cut in the transverse to flow direction

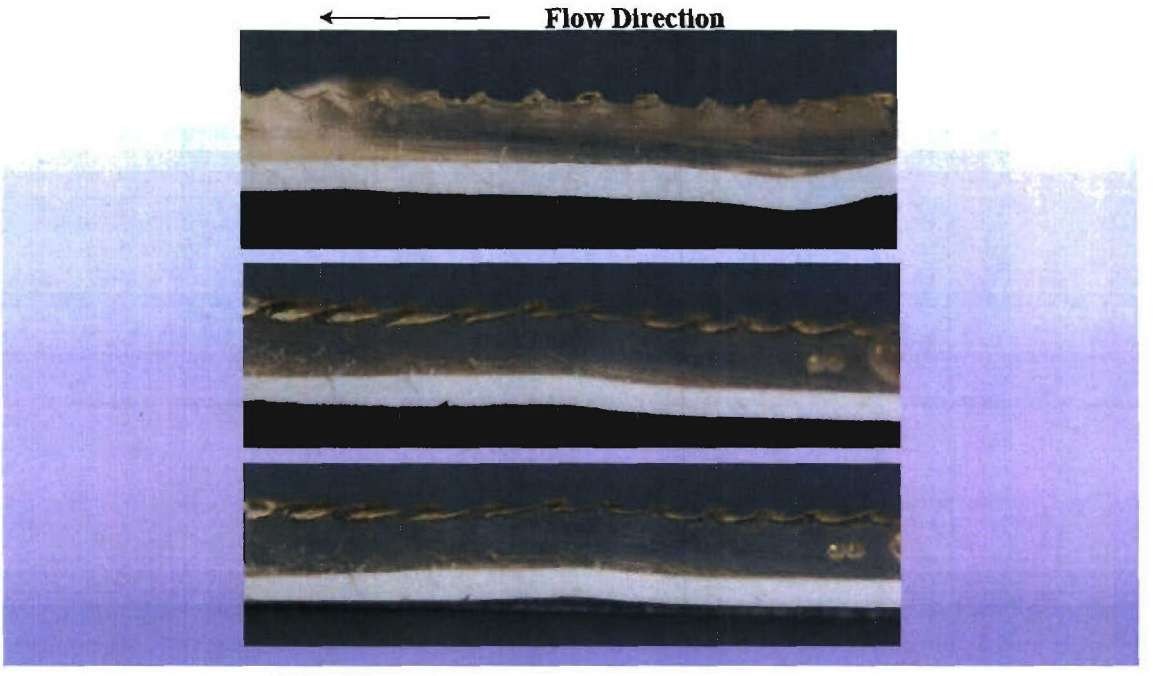

Figure 17
Distribution of the two co-extruded layers during extrusion: 0.1 in./min, cut in the parallel to flow direction

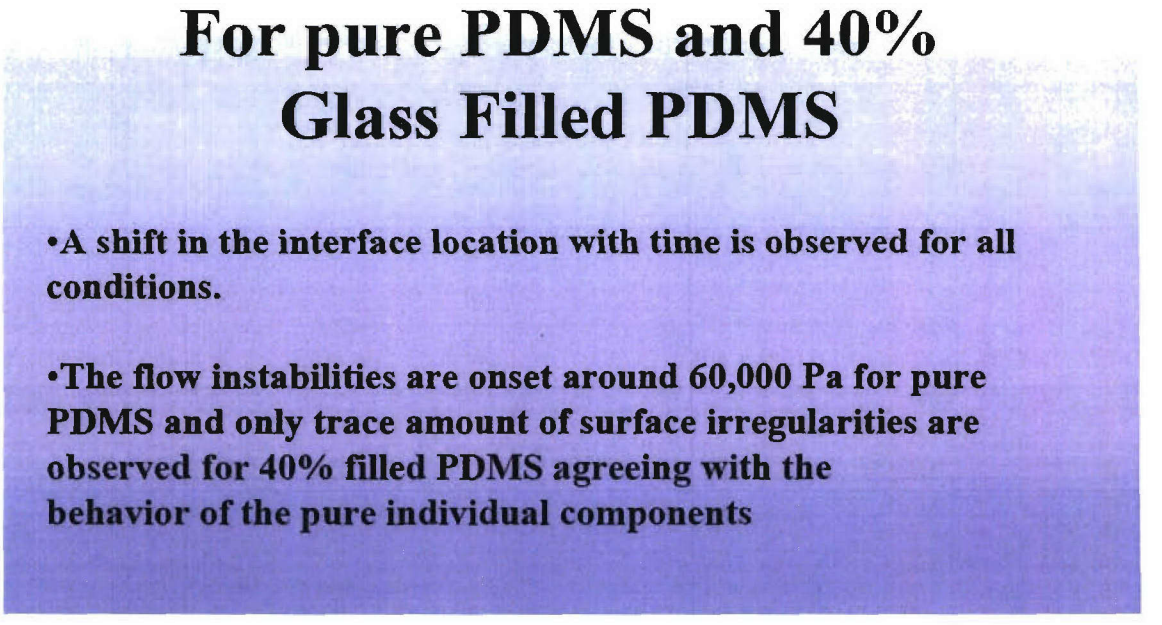

Figure 18
Summary of co-extrusion results for co-extrusion of 0 and 40%

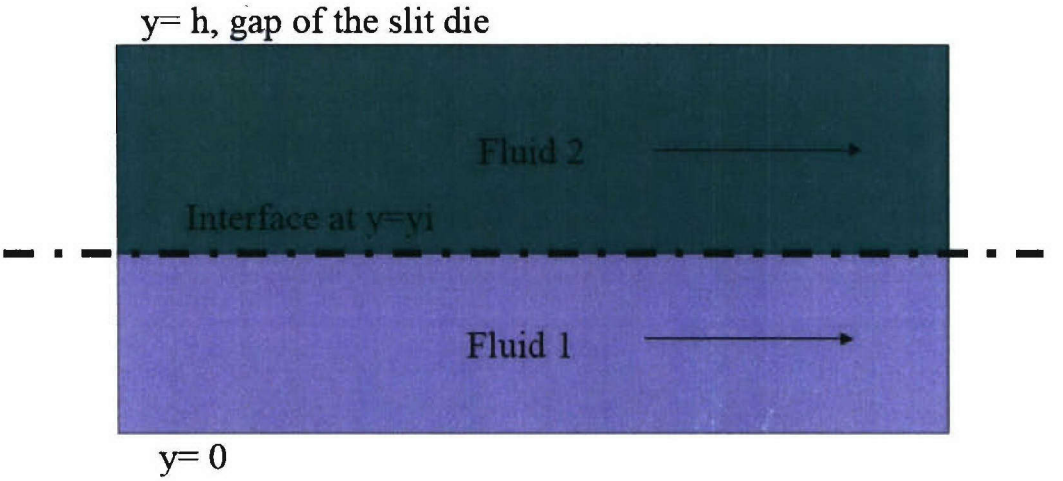

Schematic of co-extrusion of two fluids flowing side by side.

Figure 19
For the mathematical modeling: basic flow configuration for co-extrusion

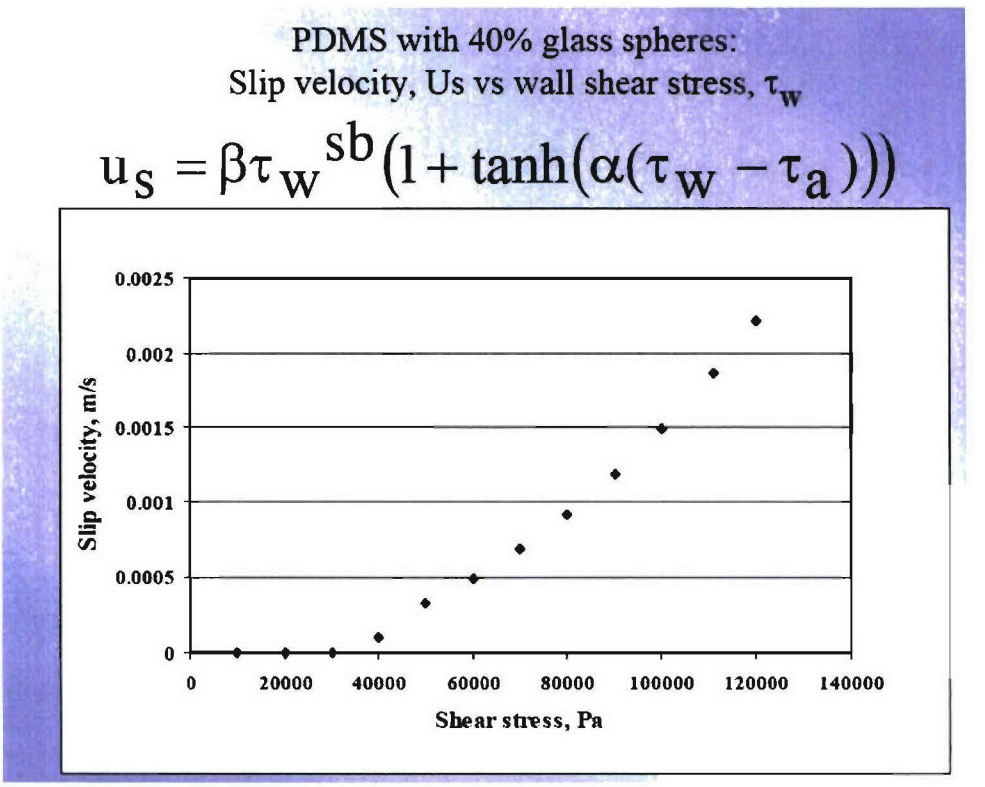

Figure 20
Slip velocity versus wall shear stress for PDMS binder with 40% by volume filler

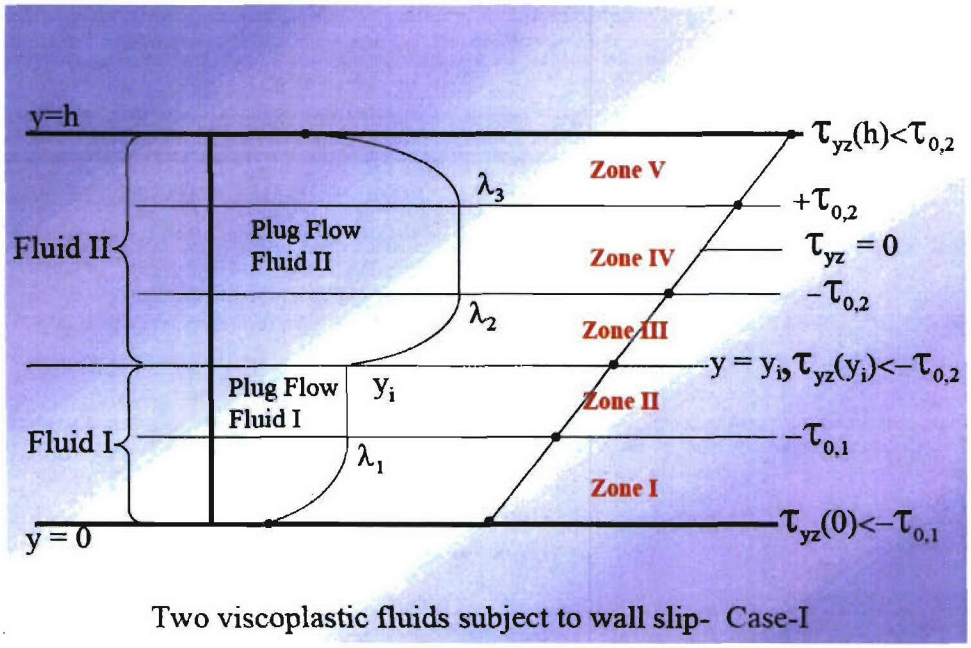

Figure 21
Shear stress distribution for case I: co-extrusion of two viscoplastic suspensions subject to wall slip

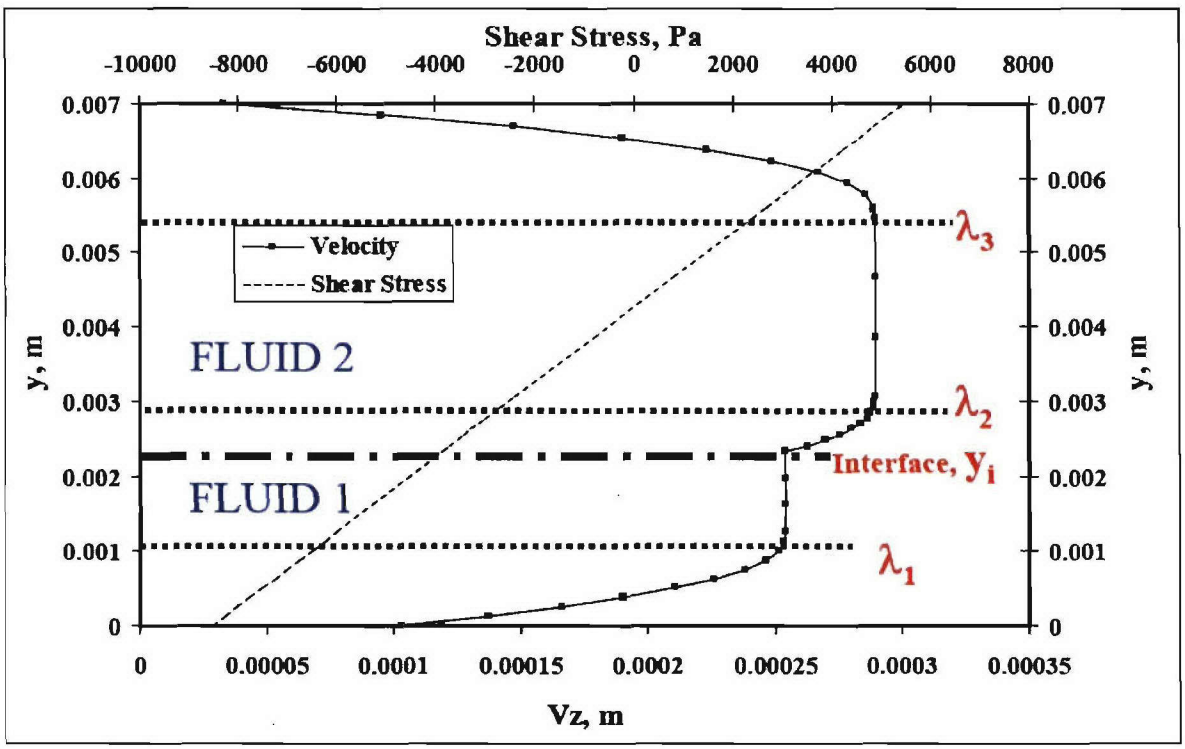

Figure 22
Velocity and shear stress distributions for case I: co-extrusion of two viscoplastic suspensions subject to wall slip

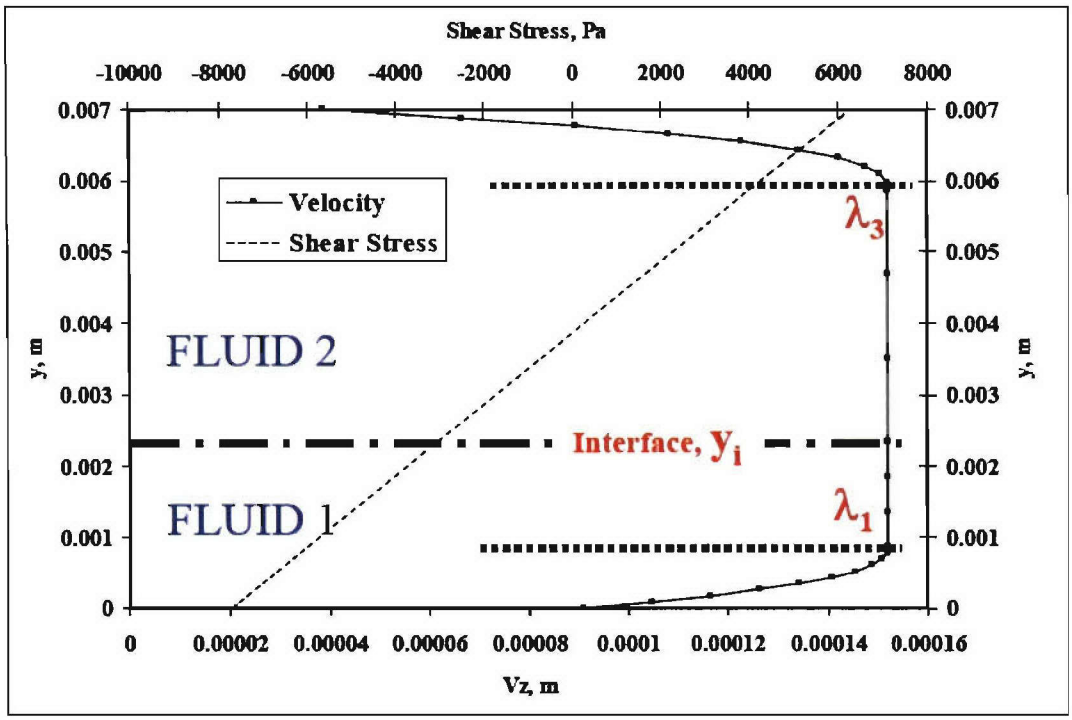

Figure 23
Velocity and shear stress distributions for case IV: co-extrusion of two viscoplastic suspensions subject to wall slip

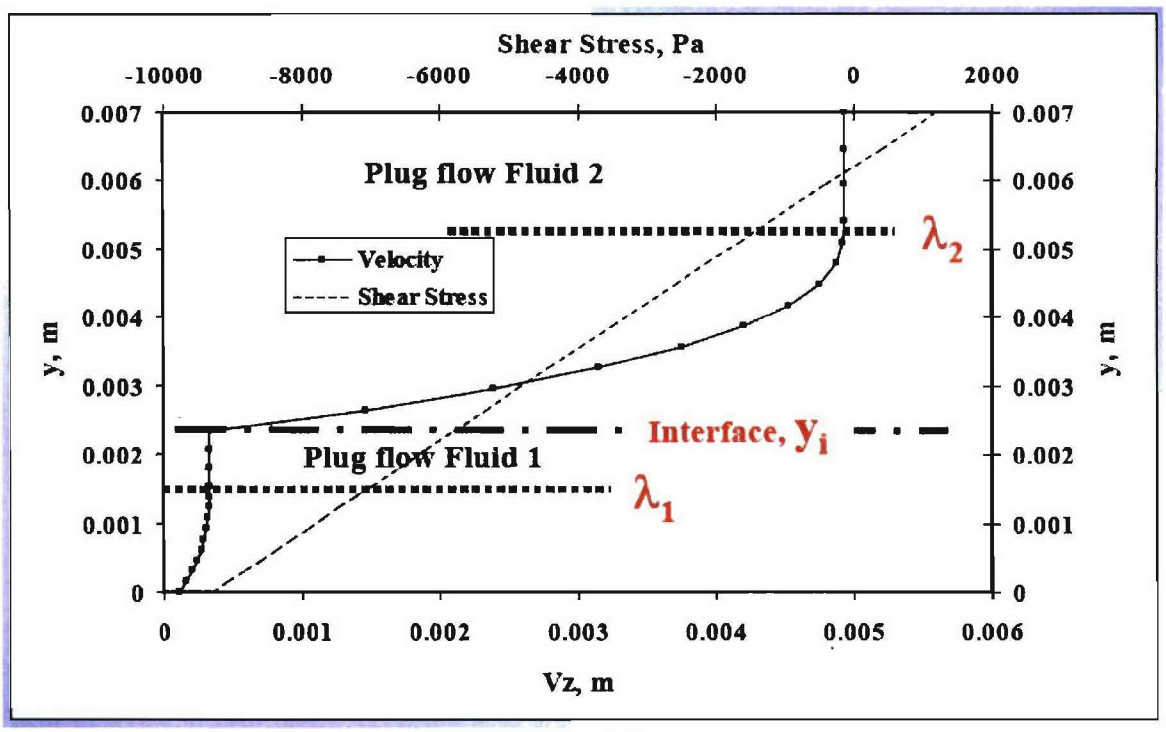

Figure 24
Velocity and shear stress distributions for case VII: co-extrusion of two viscoplastic suspensions subject to wall slip

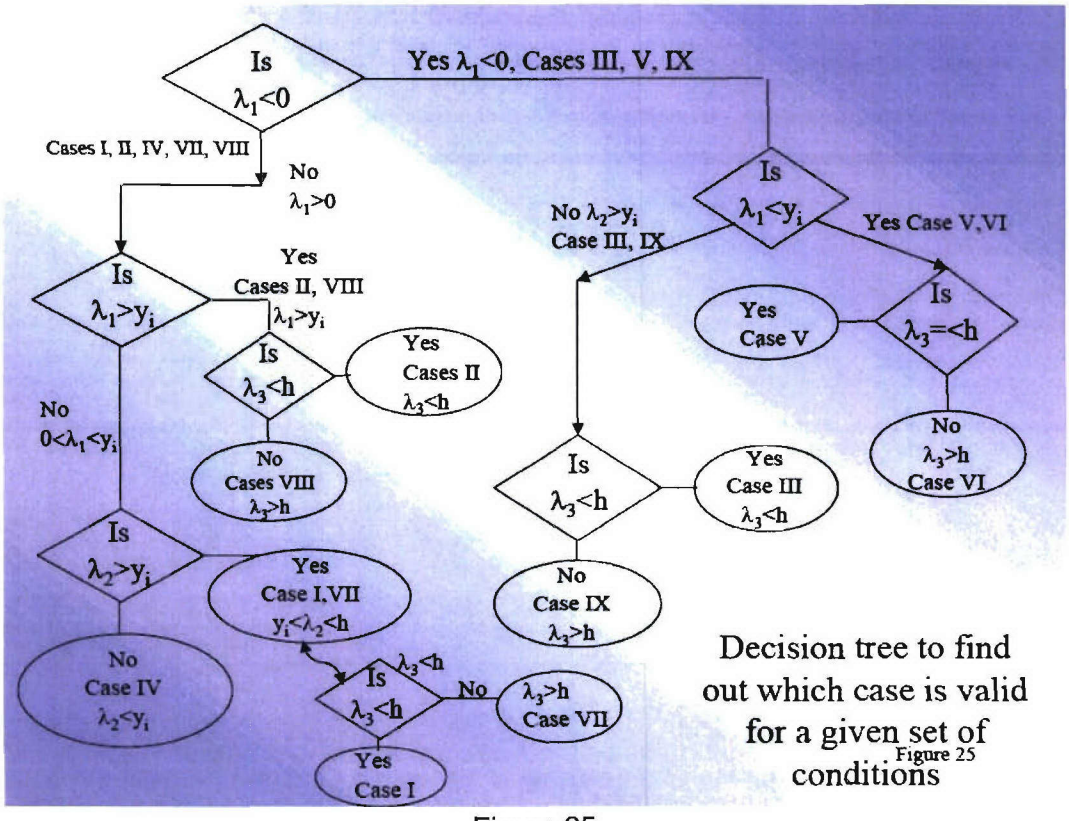

Figure 25
Decision tree for case determination for the analytical solution of the co-extrusion flow

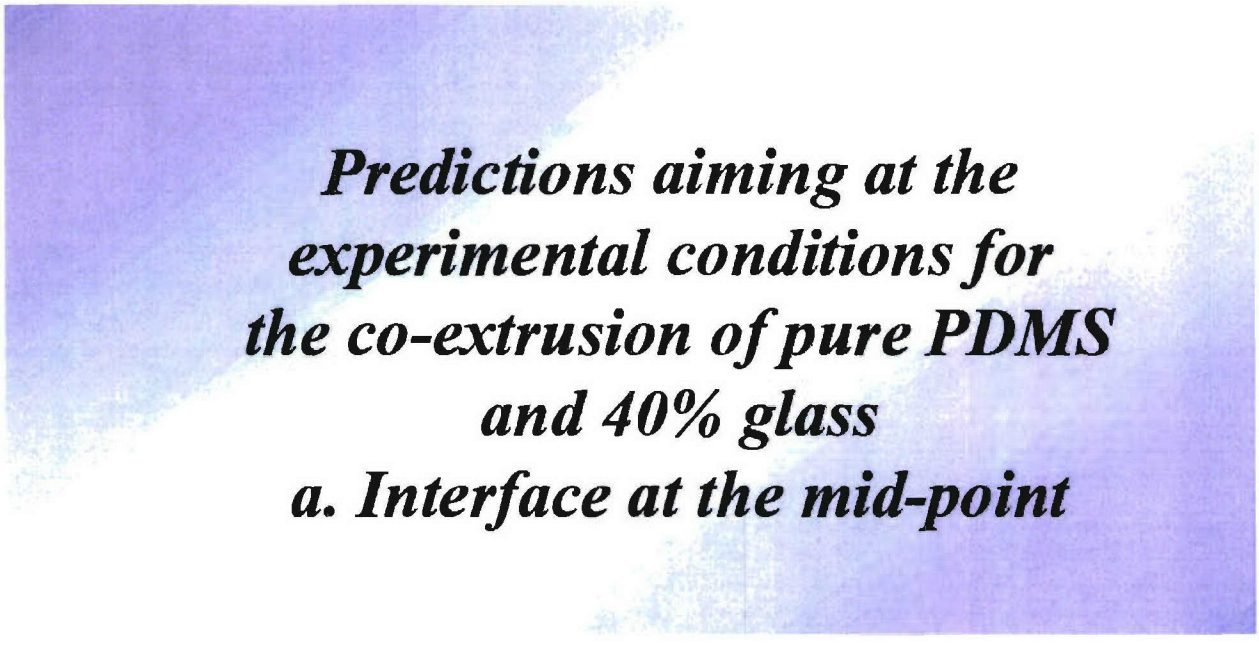

Figure 26
Predictions for co-extrusion of pure PDMS binder with PDMS with 40% filler

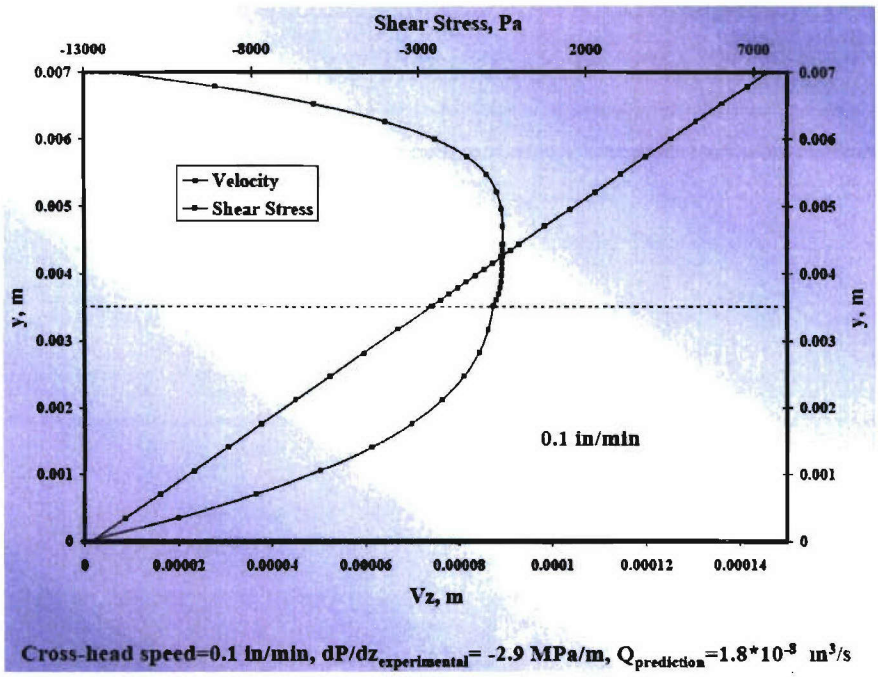

Figure 27
Predictions of velocity and shear stress distributions for co-extrusion at ram velocity of 0.1 in./min

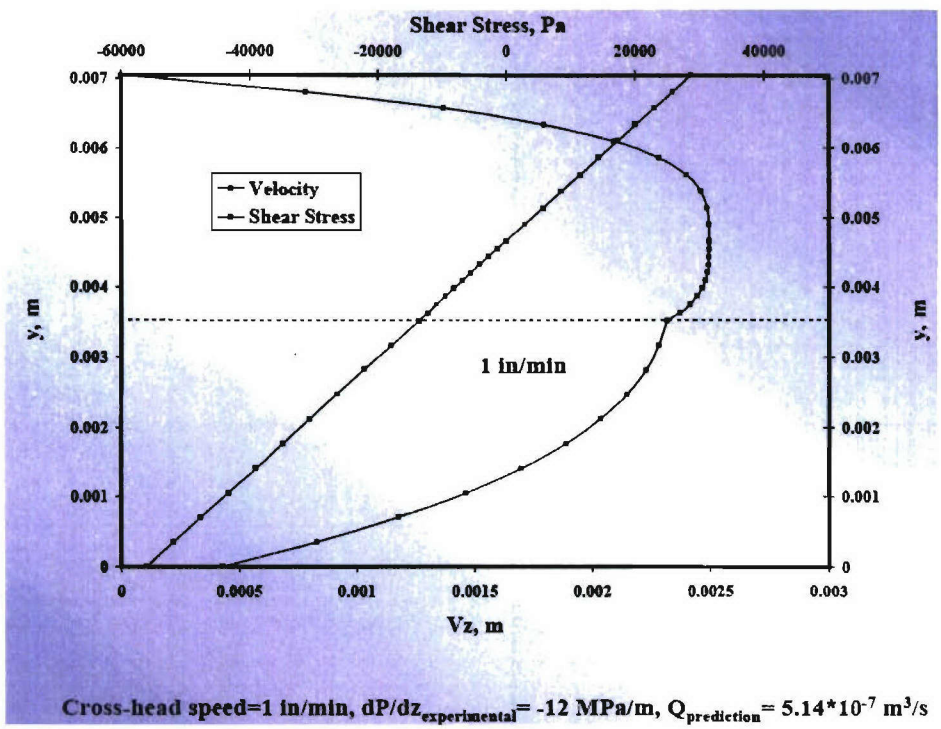

Figure 28
Predictions of velocity and shear stress distributions for co-extrusion at ram velocity of 1 in./min

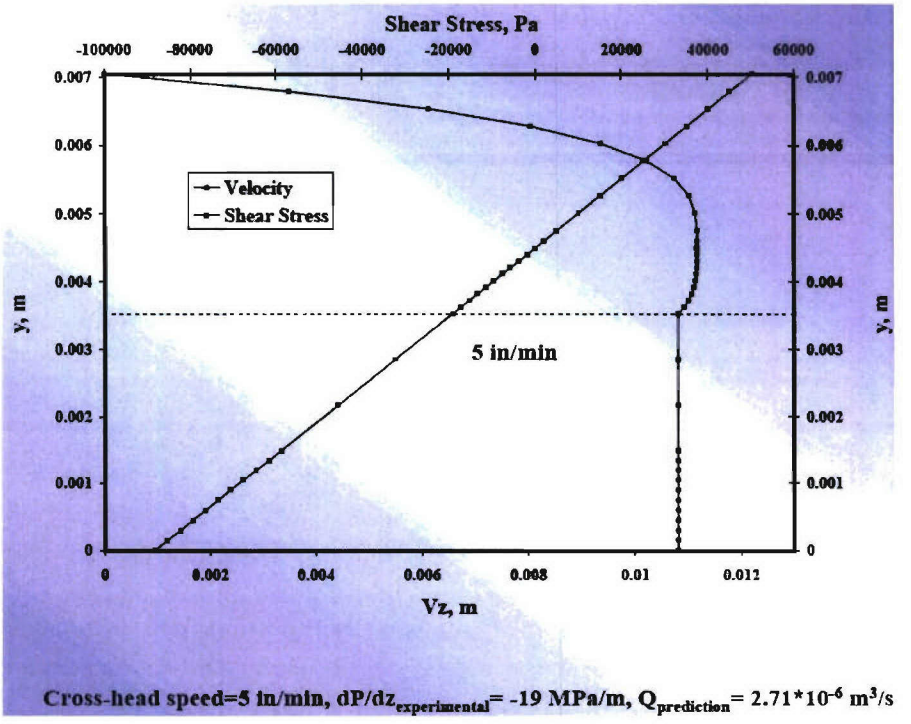

Figure 29
Predictions of velocity and shear stress distributions for co-extrusion at ram velocity of 5 in./min

Summary of experimental data and predictions for pure PDMS and 40% Glass Filled PDMS

Crosshead speed of the ram extruder inches/min	Pressure Gradient, MPa/m	Flow rate actual, m^3/s	Flow rate predicted, m^3/s
0.1	-2.9	5.40E-08	1.80E-08
1	-12	5.40E-07	5.14E-07
5	-19	2.71E-06	2.71E-06
10 (a)	-23	5.40E-06	4.00E-06
10 (b)	-26.6	5.40E-06	5.42E-06

Figure 30
Experiments versus co-extrusion theory

Predictions aiming at the experimental conditions for the co-extrusion of pure PDMS and 40% glass

b. Interface between the two fluids changing with time

Figure 31
Interface location

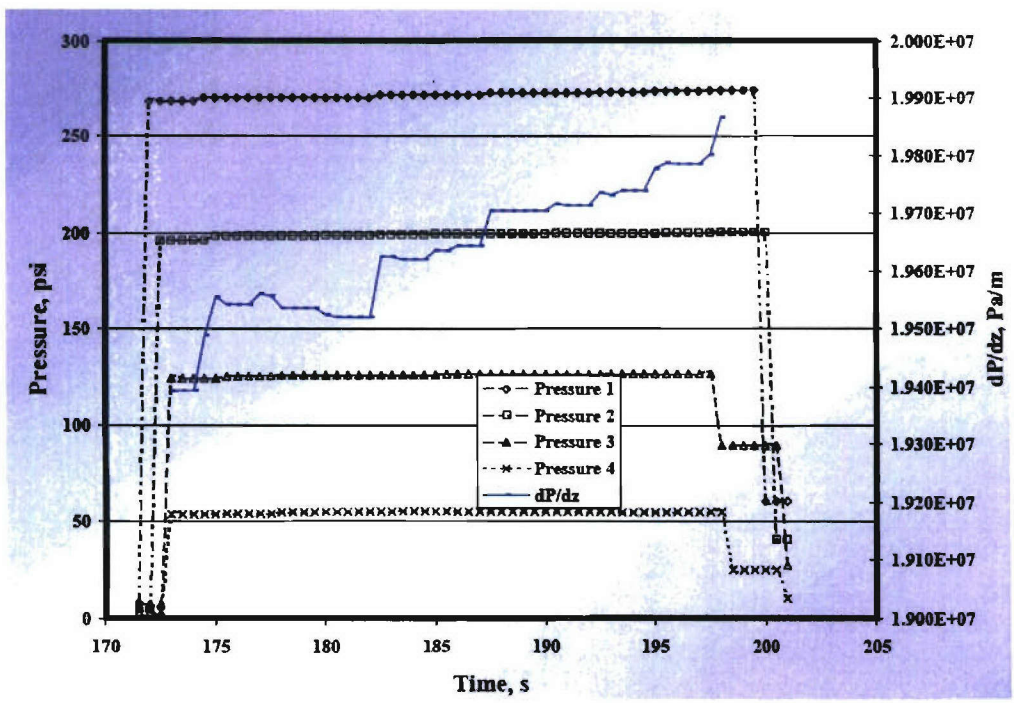

Figure 32
Pressure gradient versus time at 5 in./min

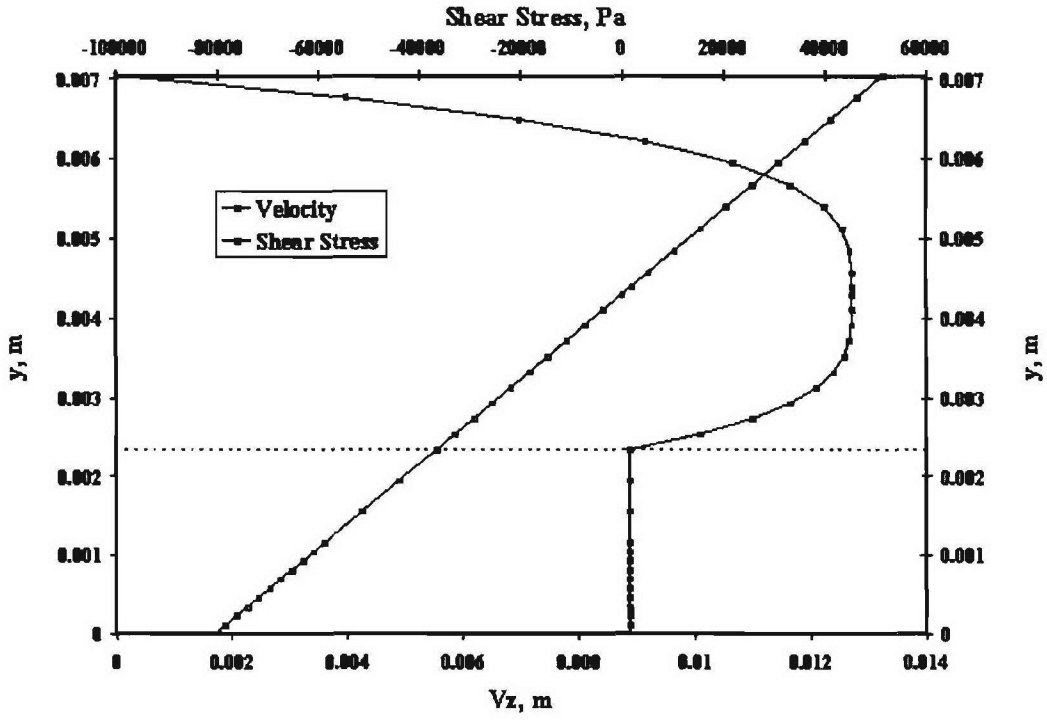

Figure 33
Velocity and shear stress profiles at 5 in./min

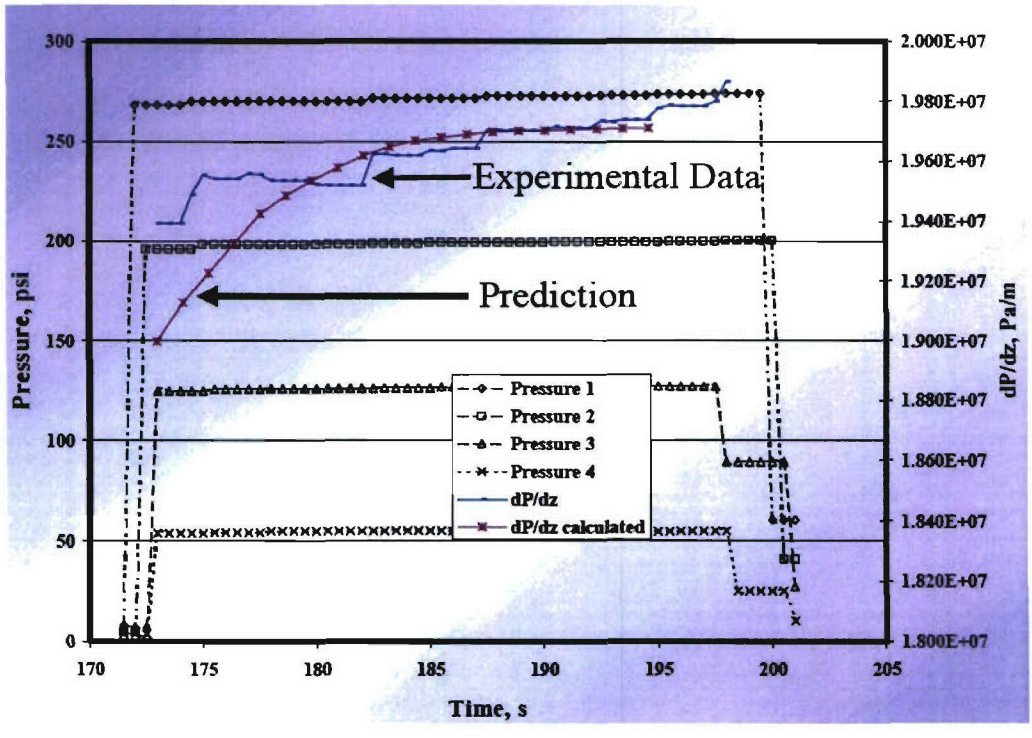

Figure 34
Experimental versus theory: pressure versus time in the slip die during co-extrusion

REFERENCES

1. Kalyon, D., "Development of Co-extrusion Technologies for Green Manufacture of Energetics," progress review presentation at SIT on 12 August 2004.

2. Kalyon, D., "Progress Report: Development of Co-extrusion Technologies for Green Manufacture of Energetics," 15 November 2004.

3. Kalyon, D.; Gevgilili, H.; Arshad, M.; and Demirkol, E., "Progress Report: Development of Co-extrusion Technologies for Green Manufacture of Energetics," 21 December 2004.

4. Kalyon, D., "Investigation of the Science and the Technology Base of Co-extrusion," progress review presentation on 25 January 2005.

5. Kalyon, D.; Tang, H.; Gevgilili, H.; Birinci, E.; Arshad, M.; Malik, M.; and Demirkol, E., "Progress Report: Development of Co-extrusion Technologies for Green Manufacture of Energetics: Experimental studies of Flow Instabilities and Mathematical Modeling of the Formation of Surface Irregularities," 18 March 2005.

6. Kalyon, D.; Gevgilili, H.; Tang, H.; Birinci, E.; Arshad, M.; Demirkol, E.; and Malik, M., "Progress Report: Development of Co-extrusion Technologies for Green Manufacture of Energetics: Experimental studies of Co-Extrusion and Comparisons with the Results of Mathematical Models of Co-Extrusion", 30 April 2005.

7. Kalyon, D., "Progress Report: Development of Co-extrusion Technologies for Green Manufacture of Energetics: Lessons learned and the issues to be addressed," 1 May 2005.

8. Kalyon, D., "Fundamentals of the Co-extrusion of Concentrated Suspensions: Ramifications on Design/Manufacture of Fast/Slow Burn Propellants", ARMY/NAVY/SIT Workshop on 3 May 2005.

DISTRIBUTION LIST

U.S. Army ARDEC
ATTN: AMSRD-AAR-EMK
AMSRD-AAR-GC
AMSRD-AAR-AEE-W, D. Park (4)
A. Eng
P. Hui
T. Manning
S. Nicolich
AMSRD-AAR-AEE-P, M. Fair
S. Moy
L. Sotsky
AMSRD-AAR-AEE-E, K. Jasinkiewicz
J. Mahon
AMSRD-AAR-EMB, D. Fair
A. Perich
Picatinny Arsenal, NJ 07806-5000

Defense Technical Information Center (DTIC)
ATTN: Accessions Division
8725 John J. Kingman Road, Ste 0944
Fort Belvoir, VA 22060-6218

Commander
Soldier and Biological/Chemical Command
ATTN: AMSSB-CII, Library
Aberdeen Proving Ground, MD 21010-5423

Director
U.S. Army Research Laboratory
ATTN: AMSRL-CI-LP, Technical Library
Nora Eldredge
Bldg. 4600
Aberdeen Proving Ground, MD 21005-5066

Chief
Benet Weapons Laboratory, AETC
U.S. Army Research, Development and Engineering Command
Armament Research, Development and Engineering Center
ATTN: AMSRD-AAR-AEW
Watervliet, NY 12189-5000

Director
U.S. Army TRADOC Analysis Center-WSMR
ATTN: ATRC-WSS-R
White Sands Missile Range, NM 88002

Chemical Propulsion Information Agency
ATTN: Accessions
10630 Little Patuxent Parkway, Suite 202
Columbia, MD 21044-3204

GIDEP Operations Center
P.O. Box 8000
Corona, CA 91718-8000

Stevens Institute of Technology
Highly Filled Materials Institute
ATTN: Prof. D. M. Kalyon
Dr. H. Gevgilili
Dr. H. Tang
Dr. M. Malik
A. Mirza
E. Demirkol
Dr. B. Greenberg
Castle Point on Hudson
Hoboken, NJ 07030

NSWC, Indian Head Division
ATTN: Rich Muscato, Code 2330D
101 Strauss Avenue
Indian Head, MD 20640-5035